# Quantifying porosity changes in solid biomass waste using a disruptive approach of water retention curves (WRC) for dry anaerobic digestion

M.A. Hernández-Shek, M. Mathieux, Laura André, P. Peultier, A. Pauss, Thierry Ribeiro

# Quantifying porosity changes in solid biomass waste using a disruptive approach of water retention curves (WRC) for dry anaerobic digestion

M.A. Hernandez-Shek[a,b,c], M. Mathieux[a,b], L. André[a], P. Peultier[c], A. Pauss[b], T. Ribeiro[a*]

[a]Institut Polytechnique UniLaSalle, EA 7519 Transformations & AgroRessources, Rue Pierre Waguet, BP 30313, F-60026 Beauvais Cédex, France.
[b]Alliance Sorbonne Université, EA 4297 TIMR UTC/ESCOM, Université de technologie de Compiègne, 60203 Compiègne cedex, France.
[c]Easymetha, 6 rue des Hautes Cornes, 80000 Amiens, France.

*Corresponding author: Thierry Ribeiro; Tel.: +33 (0) 344 06 76 11; E-mail: **thierry.ribeiro@unilasalle.fr**

## Abstract

Knowledge of the porosity distribution of biomass is crucial to understand the liquid flow through porous solid biomass treated in dry anaerobic digestion (D-AD). In this study, a novel adaptation of Water Retention Curve (WRC) analysis was validated to characterize the pore distribution of representative lignocellulosic biomasses; Cattle Manure (CM), roadside grass and corn stover. WRC analysis is composed of a drainage analysis (DA) and thermogravimetry analysis (TGA). Macro, meso and micropores values ranged from 33 to 63%, 25 to 44% and 7 to 16% for listed raw biomasses. Additionally, changes in porosity distribution of CM treated in sacrificed Leach-Bed Reactor (LBR) were quantifying; macropore volume decreased from 30.4 to 1.7% with the fiber degradation reducing considerably the permeability and increasing the solid bed compaction. The findings of this study suggest that the daily recirculated liquid volume could be progressively adapted considering the physical evolution of the solid bed.

## Keywords

Water retention curve; Porosity distribution; Dry anaerobic digestion; Solid biomass; Leach-bed reactor

27 **Nomenclature**

| | |
|---|---|
| BMP | Biochemical methane potential (NmL $CH_4$ $g_{VS}^{-1}$) |
| CCS | Chopped corn stover |
| CFD | Computational fluid dynamics |
| CHP | Combined heat and power |
| CM | Cattle manure |
| DA | Drainage analysis |
| D-AD | Dry anaerobic digestion |
| DM | Dried matter |
| DW | Drained water (kg) |
| I&S | Immersion and saturation |
| I/S | Ratio inoculum VS /substrate VS |
| K | Hydraulic conductivity (m $s^{-1}$) |
| LBR | Leach-bed reactor |
| MIM | M-mobile/IM-immobile |
| PWP | Permanent wilting point |
| RSG | Roadside grass |
| S-CM | Shredded cattle manure |
| SW | Stagnant water (kg) |
| TGA | Thermogravimetry analysis |
| TS | Total solids (%) |
| VS | Volatile solids ($\%_{TS}$) |
| $W_0$ | Initial water content in the sample (kg) |
| $W_{added\ to\ I\&S}$ | Added water to immersion and saturation (kg) |
| WHC | Water-holding capacity ($g_{water}$ $g_{DM}^{-1}$) |
| WMB | Water mass balance (%) |
| WRC | Water retention curve |
| $\varepsilon_{dry}$ | Dry porosity (%) |
| $\varepsilon_{wet}$ | Wet porosity (%) |
| $\theta_{immobile}$ | Immobile water volume (L) |
| $\theta_{mobile}$ | Mobile water volume(L) |
| $\theta_{total}$ | Volumetric total water (L) |
| $\rho_{dry}$ | Dry bulk density (kg $m^{-3}$) |
| $\rho_{wet}$ | Wet bulk density (kg $m^{-3}$) |

28

29

## 1. Introduction

Dry Anaerobic Digestion (D-AD) has already proven its efficiency in the methane recovery from lignocellulosic biomass having more than 15% of Total Solids (TS) content (Ge et al., 2016; Karthikeyan and Visvanathan, 2013; Rocamora et al., 2020). Accessibility and availability of biomass are related to the cost of collection and transportation. Biomass with higher concentration of TS involves lower transportation costs per unit of solids compared to low TS feedstocks (Brown et al., 2012). Agricultural residues, such as cattle manure and corn stover are the most common substrates for D-AD process in France (FranceAgrimer, 2016). Furthermore, yard waste, which includes grass, is a major biowaste generated from municipalities, which has become an interesting substrate for D-AD (Koch et al., 2010).

Given its simplicity and the physical characteristics of solid biomass, Leach-Bed Reactor (LBR) operated in batch is the most common technology for the anaerobic treatment and valorization of solid biomass (Riggio et al., 2017b). In this reactor, the solid biomass is irrigated with a liquid inoculum -named leachate percolating the solid bulk until being recovered at the reactor bottom. Liquid recirculation has a positive effect on the methane production, it improves the contact between the microorganisms and the solid substrate and avoid possible failures by diluting inhibitory compounds (Degueurce et al., 2016b; Kusch et al., 2012; Shahriari et al., 2011). Despite the positive effect of liquid recirculation on biogas production (Degueurce et al., 2016b; Kusch et al., 2012), there is no clear consensus between the parameters leading liquid recirculation. In general, once an operation mode is chosen (total volume, frequency, flow), this would be kept until the end of the batch operation.

Liquid percolation through the solid bed is feasible due to its porosity (Valencia et al., 2008). The total porosity of a matrix represents the fraction not occupied by solid and which is available for the liquid and gas phases. Porosity has been identified as a major element influencing the liquid distribution and the degradation efficiency of biomass in LBR (Myint and

Nirmalakhandan, 2008). Despite the importance of biomass porosity and its evolution through D-AD process, its analysis is poorly documented in literature. The physical changes of the solid bed like the loss of permeability limit the efficiency of liquid percolation to maintain the solid degradation (André et al., 2015). Unfortunately, to our knowledge, there is no method able to efficiently describe the changes in porosity distribution of the solid bed. As consequence, daily recirculated liquid volume still being established without considering the physical evolution of the solid phase.

Pore media is frequently studied by its physical relation with water (Gerke and Van Genuchten, 1993). Initially developed for the analysis of soils, two-region MIM (M-mobile/IM-immobile water) model has allowed the modeling of successive percolation and drainage operations and the presence of non-uniform flow pathways in cattle manure (André et al., 2015; Shewani et al., 2015). This model considers as mobile water the one present in the macropores and that drains rapidly into the solid bed, while water retention is assured by the micropores (immobile water). MIM model does not consider capillary region or mesopores, being this one of the highest drawbacks in its application to porous media. As a consequence, capillary effects have been responsible for differences between the experimental and numerical analysis of percolation operations in LBR treating cattle manure. Meaning the importance of considering capillary pores (mesopores) as an intermediate pore size between the macropores and the micropores. Furthermore, thermogravimetric analysis (TGA) has been used for determining the free and bound water present in biomass (Dumas et al., 2015; Garcia-Bernet et al., 2011). Some other studies have focused only on the Water-Holding Capacity (WHC) of biomass without considering the pores fraction responsible for water retention (Fernandez et al., 2020; Sanchez et al., 2019).

Biomass porosity distribution and its evolution through D-AD process remains an open question, limiting the D-AD process optimization and the liquid recirculation operation. Thus,

new methodologies need to be adapted and developed for solid biomass analysis. The Water Retention Curve (WRC) analysis is a technique relating the soil water content with the matric suction (Du, 2020; Wassar et al., 2016). This is a method frequently used to estimate the water distribution and hysteresis in soils (hygroscopic water, the capillary water and the gravitational drained water) thereby fixing water irrigation operations according to the soil type, the season and the crop water necessities. The WRC of soils is built using pressured systems as the Richards chambers or the sand pressure tables (Darwish, 2009; Jordan and Cerdá, 2010; Lavelle et al., 2014; Menéndez et al., 2005). Hitherto, no application of WRC methodology has been documented in literature for biomass, this could be explained by the fact that existed pressured chambers do not correspond to the needed volume for biomass analysis.

The aim of this work was to present a novel adaptation of WRC methodology to quickly and efficiently determine the pore distribution of solid biomass. This approach was inspired by the analysis of soils, allowed to determine the macro, meso and micropores of porous medium (Luxmoore, 1980). It integrates a first phase of immersion / saturation (I&S) of the sample with water, followed by drainage analysis (DA) and finally the thermogravimetry analysis (TGA). In the first part of this work, WRC methodology was used to characterize the pore distribution of four of the most common lignocellulosic biomasses used as substrate in D-AD; Cattle Manure (CM), Shredded Cattle Manure (S-CM), Chopped Corn Silage (CCS) and Roadside Grass (RSG). Additionally, bulk density, WHC and permeability of biomasses were determined for each biomass. Secondly, pores distribution evolution was determined from digested CM from four LBR's of 60L started up in parallel and sacrificed at different stages of the D-AD process (10, 15, 21 and 31 day). Changes in porosity distribution, fiber content of the solid phase and permeability values were quantifying and correlated. The impact of porous changes over the management of the liquid recirculation during the batch and methane production in LBR are also discussed.

## 2. Materials and Methods

### *2.1 Tested materials*

Biomass samples were collected in summer to avoid any variability due to seasonality following the protocol described by Gy (1998). No conservation of samples was undertaken, these were analyzed the same collection day.

#### *i. Cattle Manure (CM)*

CM is a mixture of cow slurry with the bedding material which is in most cases wheat straw. Two kinds of CM, non-shredded CM and Shredded CM (S-CM) were respectively collected from the farm of the Institute LaSalle Beauvais and from another farm located in Talmas (France). Non-shredded CM presented fibers of wheat straw < 20 cm. Otherwise, industrially size reduction enhanced fibers with less than 5 cm length in S-CM

#### *ii. Chopped Corn Stover (CCS)*

CCS is used as animal feed in farms. Silage fermentation of stored CCS could reduce its nutritional value, then this is considered as a farm waste needed treatment, a sample of wasted CCS was collected from the farm located in Beauvais. CCS particles have a cylindrical shape and sizes between 1.0 and 2.0 cm length.

#### *iii. Roadside Grass (RSG)*

RSG recently harvesting by cutting machines was collected in Beauvais (France). RSG was still green and fresh at the moment of collection. It was composed of fibers between 10 and 15 cm in length and <3 mm of thickness.

## 2.2 Analytical methods

### 2.2.1 Biomass physicochemical characterization

For all the experiments, the total solids (TS) and volatile solids (VS) of the raw and anaerobically digested biomass were determined (APHA, 2017). Dry and wet bulk density was determined using the mass-volume ratio in a cylindrical shape. Total dry ($\varepsilon_{dry}$) and wet porosities ($\varepsilon_{wet}$) were measured by dividing the saturated water by the total dry and wet sample weight as following (André et al., 2015; Lam et al., 2008b):

$$\varepsilon_{dry} = \frac{Added\ water\ to\ fully\ saturate\ (W_{SW})}{Weight\ of\ dry\ sample\ (W_d)} \quad \textbf{(1)}$$

$$\varepsilon_{wet} = \frac{Added\ water\ to\ fully\ saturate\ (W_{SW})}{Weight\ of\ wet\ sample\ (W_w)} \quad \textbf{(2)}$$

Van Soest fractionation allowed the determination of the hemicellulose, cellulose and lignin content (Van Soest, 1963). The biochemical methane potential (BMP) of the biomass was also measured following the methodology proposed by (Holliger et al., 2016). Experimental data will be presented as average values, in addition, the standard derivation of the results will be shown as well.

### 2.2.2 Water Retention Curve (WRC) Analysis

Adapted from the analysis performed using the Richard's chambers to determine the porosity distribution and the field capacity in soils (Darwish, 2009; Klute, 1986; Richards, 1948). The proposed approach integrates a first stage of immersion and water saturation of the biomass (I&S), followed by a second stage of drainage analysis (DA) and finally, the last stage of evaporation of residual water and measurement by thermogravimetry (TGA) (**Fig. 1**). DA and TGA allowed the quantification of water stocked in the different pores of the solid, Luxmoore, (1980) pore size classification and definitions were considered in this work, macropores would consider the pores larger than 1 mm, mesopores from 10 µm to 1 mm and micropores inferior to 10 µm. The determination of the different volumetric fractions satisfied the following equation:

$$\%Macropores + \%Mesopores + \%Micropores + \%Solids = 100\%\ volume \quad \textbf{(3)}$$

Pore distribution tests were performed in duplicate for each biomass, except the sample of CM which analysis was performed on four occasions to better statistical analysis and representativeness of the proposed methodology.

*2.2.2.1 Sample preparation*

The medium to be analyzed is gently placed in a cylindrical plastic laboratory constructed permeameter (internal diameter 0.26 m, total height 0.25 m) until reaching about 0.2 m solid height. In order to avoid sample volume changes during the next step, the initial sample volume was fixed using a metallic aperture grill on the top of the sample.

*2.2.2.2 Immersion and Saturation (I&S)*

Tap water was gently injected from the bottom until the solid bed was completely filled with water. When water levels decreased for biomass absorption, more water was added until the top grill. At this stage wet porosity was determined using Eq. **2**. The system was maintained closed for two hours to make the wetting and saturation process more efficient (Fernandez et al., 2020; Shewani et al., 2015). At this stage, it is assumed that total biomass porosity was completely filled with water, and biomass achieved the maximum WHC.

*2.2.2.3 Draining analysis (DA)*

Once the submerged time ended, water was gravitationally drained from the permeameter bottom for 24 h. Drained water mass was measured using a HD150 balance (My Weigh, United States, precision ± 20 g). The weight values were taken every 5 seconds during the first minute and then every minute until completing the first 10 minutes of DA. From this moment, data was registered each 10 min until the first hour and from there each hour to the end of the DA. Disruption of linear behavior of recovered water with time in the DA indicated the limit between the macropores and the rapid mesopores. According to Luxmoore (1980) in macropores drainage may occur very rapidly with the presence of surface ponding or perched water, while

rapid mesopores or capillary flow may occur without the of theses last. Thus, once the slope of drainage drastically changed, the recovered water concerned rapid mesopores flow.

*2.2.2.4 Thermogravimetric analysis (TGA)*

Once the previous test was achieved, 20 g of remaining solid was collected and placed on an aluminum pan (diameter 10 cm). Then, the sample was introduced into a moisture weight Mark 160Top-Ray (BEL Engineering). Water evaporation was carried on at 105°C and sample weight loss data were registered each second using a RS232 port connected to a PC (Dumas et al., 2015; Garcia-Bernet et al., 2011). Samples weight data was analyzed using the moisture derivation of the Savitzky-Golay filter in Scilab 6.0 (Savitzky and Golay, 1964). This derivation allowed to identify the limit between the water present in mesopores and water present in the micropores of biomass. The Savitzky-Golay filter derivative of the resulted curve from the evaporation test of the RSG sample is illustrated in **Fig. 2**. At first, a period of increasing temperature is depicted until α, this is succeeded by a constant water evaporation until β, the fraction of water evaporated since the beginning of the test until β refers to water presented in capillary or mesopores.

*2.2.3 Water mass balance in WRC analysis*

Draining and evaporation test results allowed the construction of the experimental WRC for each biomass; DA allowed the quantification of water present in macropores and in rapid mesopores, whereas the TGA allowed the quantification of water stocked in capillaries (mesopores) and water very attached to the biomass, these pores spaces were considered as micropores. Water mass balance analysis was used to validate the results of WRC methodology using the following equations:

$$\%\ Water\ mass\ balance\ (WMB): \frac{Drained\ water\ (DW) + Stagnant\ water\ (SW)}{Water\ in\ sample\ (W_0) + Added\ water\ (W_{added\ to\ I\&S})} \quad \textbf{(4)}$$

With:

$Water\ in\ sample\ (W_0)$ : initial water weight in the sample determined by multiplying the initial biomass weight by the humidity.

$Added\ water\ (W_{added\ to\ I\&S})$: added water to achieve immersion and saturation of the sample

$Drained\ water\ (DW)$: drained water weight once DA is complete (Macropores and rapid mesopores volume)

$Stagnant\ water\ (SW)$: water present in the samples after DA determined by multiplying the remaining mass by the humidity determined by TGA (Slow mesopores and micropores volume)

### *2.2.4 Determination of Mobile and immobile water volume fractions*

In this work mobile ($\theta_{mobile}$) and immobile ($\theta_{immobile}$) water volume fractions were determined from the previous mass balance. These fractions have been determined from the total and added water to achieve I&S.

$$\frac{\theta_{mobile}}{\theta_{added}} = \frac{DW}{W_{added\ to\ I\&S}} * 100 \quad \textbf{(5)}$$

$$\frac{\theta_{immobile}}{\theta_{added}} = \frac{W_{added\ to\ I\&S} - DW}{W_{added\ to\ I\&S}} * 100 \quad \textbf{(6)}$$

$$\frac{\theta_{mobile}}{\theta_{total}} = \frac{DW}{W_{added\ to\ I\&S} + W_0} * 100 \quad \textbf{(7)}$$

$$\frac{\theta_{immobile}}{\theta_{total}} = \frac{SW}{W_{added\ to\ I\&S} + W_0} * 100 \quad \textbf{(8)}$$

### *2.2.5 Hydraulic conductivity*

The permeameter described in section 2.2.2 was used to determine the permeability of each sample. The same procedure of filling was performed and tap water was added until the permeameter limit (0.25 m), then, water was allowed to percolate the sample and the changes in water level with time were recorded using a cell phone (one plus 6.0). Video was analyzing using DaVinci software in order to better estimate the time of the water descent. The following equation allowed the determination of the water permeability (m $s^{-1}$).

$$K = \frac{H_{biomass}}{t} * Ln\left(\frac{h_{o\_water}}{h_{f\_water}}\right) \quad \textbf{(9)}$$

Where $H_{biomass}$ is the biomass height (m), t is the recorded time (s), $h_{o\_water}$ and $h_{f\_water}$ were the initial and the final water height respectively (m).

*2.3 Inoculum characterization*

Liquid inoculum was obtained from a previous D-AD cycle in a 500L batch digester fed with CM operated under mesophilic temperature (37°C) for two months. Thereafter, it was stored in drums at room temperature for one week. Before sampling for D-AD experiments, the inoculum was homogenized. TS content was measured at 1.9% and the VS averaged 42.5%$_{TS}$. The initial pH was 8.4 and the VFA/alkalinity ratio was measured at 0.125.

*2.4 Dry Anaerobic Digestion of CM in Sacrificed LBR's*

Given its highlighted importance in agricultural methane production, CM was chosen as a substrate for D-AD process to validate and compare the results of this study with literature. In order to follow physical changes of biomass with the already proposed WRC method. Four batch reactors with liquid recirculation were started in parallel, and each was sacrificed at different stages of degradation according to the typical biogas flow behavior in a batch D-AD digester treating CM (André et al., 2015). The first batch reactor corresponded to the initial conditions of the CM before anaerobic digestion (day_0). The second reactor corresponds to the first peak of methane production (day_10), third reactor corresponds to the methane production valley founded between days (day_15), the fourth reactor was sacrificed once reaching the second peak of methane production (day_21) and finally, the fifth reactor was sacrificed when biogas flow would decrease until the batch end (day_31).

The four reactors used in this study were made of polyethylene; the internal diameter and the total height were 39 cm and 50 cm, respectively, for a total volume of approximately 60 L. A mesh (5 mm holes) placed at the bottom avoided solid blockage of liquid phase pipes

236 recirculation. Twenty-one kilograms of CM were gently placed in the reactor using hands,
237 subsequently, 22 kg of inoculum (liquid phase) was added obtaining a ratio Inoculum/Substrate
238 (I/S) of VS content equal to 0.05.

239 Loaded reactors were hermetically sealed and a thermostatically controlled water bad allowed to
240 keep mesophilic temperature (37°C) during all the batch duration. Approximately 40 L of the
241 liquid phase was daily recirculated (2 min each 2 h with a flow rate of 100 L $h^{-1}$) using
242 MasterFlex peristaltic pumps. A valve in the liquid phase circuit enabled samples to be taken for
243 analysis. Biogas production was continually measured using drum gas meter TG5 (Ritter,
244 Germany), biogas composition ($CH_4$, $CO_2$ and $H_2$) was monitored daily by a MGA300 multi-gas
245 analyzer (ADC Gas Analysis Ltd, Hoddesdon, United Kingdom).

246 In order to follow and control the anaerobic digestion process, the liquid phase was sampled and
247 analyzed on a daily basis. The pH and the conductivity were measured using Mettler Toledo
248 (Switzerland) SevenEasy$^{TM}$ $S_{20}$. The buffer capacity and the volatile fatty acid concentration
249 (VFA) were determined by two acidification steps using sulphuric acid. The first acidification
250 down to pH 5.0 allowed the buffer capacity to be determined, and the second acidification down
251 to pH 4.4 allowed the quantity of volatile fatty acids to be determined. These analyses were
252 carried by means of an automatic titrator $T_{50}$ (Mettler Toledo, Switzerland).

253 Once each reactor was sacrificed, physical characterization of the solid phase was performed
254 according section 2.2.1. In order to minimize any structural changes of the samples for WRC
255 analysis, similar core drilling procedure performed in soils was used, representative sampling
256 amount (around 3 kg) of the solid was taken using a sharpened cylinder and carefully introduced
257 into the permeameter. Finally, Pearson linear correlation analysis was performed to assess the
258 significance and correlation between the pore distribution with TS content, VS content, the fiber
259 content, the bulk density and permeability.

## 3 Results and Discussion

### *3.1 Biomasses physical characterization*

Physical properties of four of the most common biomasses treated by D-AD process were measured in this section (**Table 1**). Physical properties such as the TS, the VS and the bulk density are essential parameters for D-AD because they determine the loading of biomass, and consequently the methane yield per volume of reactor (Caicedo et al., 2017; Møller et al., 2014). For tested biomass, TS values ranged from 14.5 and 20.1 % except for corn silage with 37.7% TS (**Table 1**). These values of TS are in the range of lignocellulosic biomass treated by D-AD process (Brown et al., 2012; Rocamora et al., 2020; Sawatdeenarunat et al., 2015). Biomass is considered as a spongy material; it means that according to their particle size, biomass can integrate and absorb high water quantities inside the vegetal tissues, hence, dry biomass is frequently used as bedding by livestock activities. Biomass WHC increase with size reduction due to an increase of the contact surface of biomass (Dumas et al., 2015; Fernandez et al., 2020). This fact was observed when comparing CM with S-CM, the WHC were 6.7 ± 0.2 and 7.4 ± 0.2 $g_{water}\ g_{DM}^{-1}$ respectively.

Bulk density and porosity depend on the particle shape, size and orientation, the particle specific density, the particles size distribution, the moisture content and the applied pressure (Lam et al., 2008a). In shredded CM, the fibers size reduction and a larger presence of feces increased the humidity, as a consequence, higher wet and dry bulk density values compared to non-shredded CM (**Table 1**). Initial bulk density has been identified as a key factor in the anaerobic treatment of municipal solid waste in LBR, indeed, over 1000 kg $m^{-3}$ inhibition of methane production was observed (Caicedo et al., 2017). Degueurce et al., 2016a have reported similar values of non-shredded CM bulk density for samples collected during the winter, they have used the "Schaub-Szabo" device to measure the evolution of the bulk density with the material height

284 from 0.2 to 2.2 m, their results suggests an increase in bulk density from 311 to 577 kg $m^{-3}$ with
285 the material deep, meaning an increase of 85% of the bulk density.

286 Biomass porosity values are shown in **Table 1**, the dry porosity concerns the total porosity after
287 drying the sample at 105°C, whereas the wet porosity refers to the total available porosity of the
288 sample at the moment it was collected. Total dry porosity values were around 90% for all
289 biomass, according to Jordan and Cerdá (2010), total porosity is very high over 60% and too
290 low under 30%. Similar values of dry bulk density and dry porosity have been presented by
291 André et al. (2015) treating non-shredded CM, however, values of dry porosity barely changed
292 between the initial CM and the digestate. In consequence, total dry porosity by itself does not
293 represent the physical changes of CM treated in D-AD.

294 Wet porosity values showed higher variability than dry, meaning that water presence and its
295 distribution may play an important role in the porosity volume of biomass and in the hydraulic
296 behavior. Initial moisture in biomass samples indicates that a portion of porosity is already water
297 filled. Comparing S-CM with non-shredded CM, size reduction enhanced important physical
298 changes in the biomass, reducing wet porosity values from 51.7 ± 1.3% to 18.6 ±1.7%.
299 Moreover, despite the differences in particle size and shape and TS content, CCS and RSG
300 presented similar values of porosity and bulk density, both dry and wet. Based on the previous
301 results, it appears that physical parameters present a high variability given their interdependent
302 correlation, more research should be performed in order to establish detailed physical models
303 than the existed ones to easily determine the potential biomasses that could be treated in LBR
304 for methane recovery.

305 *3.2 WRC analysis of biomass for pores distribution determination*
306 As describe before, total porosity can be distinguished according to its function and relation with
307 water (**Fig. 1**); macropores are the larger ones and allow the rapid percolation of water and the
308 presence of a gas phase in the biomass. Next, the mesopores ensure the presence of capillary

309 water, they can be divided into rapid and slow mesopores. Finally, the micropores water volume
310 concerns vicinal or bound water. Water stocked in mesopores can be removed by mechanical
311 dewatering, whereas the water in the micropores can be only withdrawn using heat. **Fig. 3**
312 illustrates the experimental WRC for each tested biomass, this analysis is composed of two sub-
313 sequential analyses; the DA and the TGA giving as result the porosity distribution for each
314 biomass, macro-, meso-, micropores and solid percentages of the total biomass bulk volume.
315 Macropores were represented with green color, mesopores with yellow, micropores in blue and
316 solid fraction in gray.

317 *3.2.1 DA: Macropores and rapid mesopores volumes*

318 According to the proposed WRC methodology, the water volume present in macropores
319 channeling would flow with a linear behavior in the first seconds of the DA, a change in this
320 linear behavior indicates the macropores water stock depletion, from this point, recovered water
321 in the next hours for DA concerns the water stocked in rapid mesopores channeling (dash yellow
322 line). According to Luxmoore (1980), macropores drainage occurs very rapidly once DA start,
323 while, rapid mesopores drainage includes slow capillary water flow without the presence of
324 pounding or perched water in the solid. The DA was maintaining for 24 hours in order to ensure
325 maximal water recovery from rapid mesopores. Time log-scale was useful to represent the
326 draining behavior since higher changes are expected in the first minute of the test.

327 Similar values of macropores volume for CCS and RSG were measured, 58.0% and 62.0%
328 respectively (**Fig. 3a** and **b**). However, the draining was faster for the RSG than for the CCS,
329 this explains the slight difference between the macropores slopes of these two biomasses. Even
330 if these samples have similarities in their physical properties, the solid particle shape is different
331 affecting the shape of pores, as a consequence, differences in the drainage velocity have been
332 observed. Further research is necessary in order to fully determine the effect of particles shape
333 on the pores shape structure for solid biomass. Otherwise, WRC results of S-CM presented low

334 macropore volume (1.1%) affecting the amount of water recovered in DA (**Fig. 3d**). Contrary to
335 S-CM (**Fig 3c**), non-shredded CM had better macropores structure with 30.4%. As indicated
336 before, rapid mesopores volume was determined after the linear macropores draining for each
337 biomass, for RSG, CCS and CM, the rapid mesopores volume was 7.9%, 8.43% and 5.32%
338 respectively, whereas for S-CM only had 0.31% for this type of pore channeling.

339 The presence of macropores is linked with the permeability values of matter (**Table 1**). In
340 biomasses with lower values of macropores, lower values of permeability have been observed.
341 Considering the S-CM, the measured permeability value (**Table 1**) was only $1.2 \cdot 10^{-8}$ m $s^{-1}$, this
342 was very low compared to the other tested biomass with values from $8.6 \cdot 10^{-4}$ to $1.3 \cdot 10^{-3}$ m $s^{-1}$.
343 Concentrated biomasses with lower values than $10^{-4}$ as the S-CM could not be an indicated
344 substrate for D-AD process with liquid recirculation, because water can barely infiltrate the
345 biomass and very low percolation rate is observed. This kind of biomass could be subject better
346 of a reactor type different from LBR.

347 Finally, the DA allowed the determination of the WHC at 24 h of drainage of biomasses.
348 Compared to other biomasses, S-CM was the biomass with higher WHC value with (7.4 ± 0.2 g
349 water /g TS) (**Table 1**). WHC values for CM, RSG and CCS were 6.74, 7.35 and 4.08 $g_{water}$ /g
350 $_{TS}$ respectively. Fernandez et al. (2020) showed similar results of WHC for samples of CM
351 before and after industrial size reduction. Consequently, biomass WHC is affected by the same
352 parameters determining physical properties described before.

353 *3.2.2 TGA: Slow mesopores and micropores volumes*

354 The next step in the proposed methodology concerns the TGA, here a sample of the remained
355 solid of DA was analyzing using a thermogravimetric balance in order to quantifying the slow
356 mesopores and the micropores volume. Whilst the former refers to water trapped inside crevices
357 and interstitial spaces, the latter made emphasis on the hydration water (water chemically bound
358 to the particles) and the vicinal or surface water (monolayer and multilayer) (Garcia-Bernet et

al., 2011). The limit between mesopores and micropores for RSG sample is depicted in **Fig 2**. The fraction of water evaporated since the beginning of the test until β refers to water presented in capillary or mesopores which is less influenced by the solid particles. This fraction of water plays a key role in D-AD since it determines the available water for microorganisms (Garcia-Bernet et al., 2011). As can be seen, β mark a sudden change of the water evaporation derivative at time 480 seconds, it means that the constant water rate evaporation ended and from this point the remaining humidity is harder to evaporate, thus a reduction in the evaporation rate indicating the limit between mesopores and micropores. Water evaporated from β to ψ is considered as micropores volume water, given its strong relation with the solid, this water fraction is not available from metabolic activities of microorganisms (Abbassi-Guendouz et al., 2012; Garcia-Bernet et al., 2011).

The results of TGA for each biomass are also depicted in **Fig. 3**. Total mesopores volume fraction concerns the sum of the volume of rapid mesopores determined in DA and the slow mesopores quantifying using the TGA. Similar values were obtained for the mesopores volume of RSG and CCS with 26.4 ± 0.8% and 25.2 ± 0.3% respectively. In contrast, CM samples presented more significant number of mesopores and micropores than RSG and CCS, the presence of animal slurry would be responsible for these higher values. S-CM achieved 64.9 ± 3.6 of mesopores volume, while for CM this fraction represented 44.4 ± 3.4% of the total porosity. As can be seen, in S-CM the macropores volume was transformed in mesopores volume due to the size particles reduction. Mesopores volume could include dead-end pores and isolated or closed pores of the solid volume (Nishiyama and Yokoyama, 2017; Yokoyama and Takeuchi, 2009), in these pores water and gas could be stocked and limited mass transfer may enhance local inhibition of D-AD process .

Similarities between the values of solid and micropores volumes percentages for all biomasses were observed (**Fig 2**), this could be explained due to micropores are inside the solid fraction

384 and on its walls surface; indeed, SEM images have already allowed the observation of the
385 internal micropore structure of wheat straw fibers (Han et al., 2012). In S-CM, size reduction
386 increased the microporosity volume by the creation of more surface of solid, thus higher WHC.
387 Otherwise, compared with the other tested biomasses, RSG obtained the lower value of
388 micropores 6.8% and solid volume fraction 4.8%, this could be due to that sample was analyzed
389 fresh and green, just after harvesting; thus, the vegetal structures were not degraded and were
390 naturally filled with water and less water absorption took place while the test was performed. It
391 seems that biomass sponginess increases by drying due to a partial irreversible collapse of pores
392 and the creation of larger water absorption pores (Meng et al., 2013).

393 *3.2.3 WRC analysis Vs MIM model*

394 In the double porosity MIM model, the volumetric water content is assumed to be divided into
395 two distinct volumetric regions; mobile ($\theta_{mobile}$) also called macropores and immobile ($\theta_{immobile}$)
396 known as micropores. In order to compare WRC analysis with previous works using double
397 porosity model and setting the advantages of the proposed methodology, mobile ($\theta_{mobile}$) and
398 immobile ($\theta_{immobile}$) water volume fractions have been determined from the total water and the
399 added water to achieve I&S. $\theta_{mobile}/\theta_{added}$ refers to the drained water after 2 hours over the added
400 water, thus the sum of macropores and rapid mesopores volume, controversy, $\theta_{immobile}/\theta_{added}$
401 indicate the stagnant water fraction stocked in slow mesopores and microporosity over the added
402 water.

403 Analysis of CM gave as results 60.0 ± 3.6% of $\theta_{mobile}/\theta_{added}$ and 40.0 ± 3.6% of $\theta_{immobile}/\theta_{added}$;
404 similar values were reported by André et al. (2015) as macro and microporosity, 64% and 36 %
405 respectively, using modeling of tracer tests. MIM model limitations have been observed since it
406 does not consider the initial absorbed water by the sample before the test in which diffusion and
407 convection of the tracer is more difficult. As a consequence, inconsistent results in the first 21
408 days of D-AD process indicates difficulties in determining the pore distribution of digested

409 samples of CM. In WRC analysis, the initial volumetric was including in the mesopores and
410 micropores volume calculation, this could represent an advantage over MIM model.

411 In another work, Shewani et al. (2015) using double region porosity model have measured
412 values from 18 to 50% for macroporosity, 42 to 70% for microporosity and 8 to 12% for the
413 solid volume of CM with different compaction levels. In this work, using the same calculation
414 proposed by the previous authors for CM with 18.59 ± 0.43 %TS, values in the same range of
415 measure were determined at 30.5 %, 60.5% and 9% respectively for macroporosity,
416 microporosity and solid volume, Even though Shewani et al. (2015) have for the first time given
417 values for macropores, micropores and solid volume, their method for porosity distribution
418 does not consider the mesopores or capillary volumes. Consequently, this fraction of pores was
419 responsible for differences between experimental and calculated drainage results using
420 Computational Fluid Dynamic (CFD) tool. The proposed WRC analysis included the mesopores
421 or capillary volume and offer a better pore distribution information for future studies of these
422 kinds of porous media.

423 In order to measure the applicability and accuracy of WRC analysis to determine the water
424 distribution in biomass samples, water mass balances (WMB) were performed using Eq. **4** (see
425 **Table 1**) obtaining higher values than 96.7 ± 0.1%. WRC methodology coupled with tracer tests
426 and digital volumetric imaging could be powerful tools in the understanding of the pore
427 distribution network evolution of treated biomass in D-AD. Finally, the effect of pore
428 distribution, tortuosity and preferential flow pathways on liquid recirculation could be fully
429 simulated using CFD (Vallabh et al., 2011).

430 *3.3 Dry Anaerobic Digestion of CM in Sacrificed LBR*

431 In the previous section, the use of WRC analysis has successfully quantifying the pores
432 distribution of several biomasses. This section presents the results of the changes in porosity
433 distribution of anaerobically digested CM from days 10, 15, 21 and 31 have been sampled from

60 L sacrificed LBR's. Reactor mass balances between the inlet and the outlet ranged from 93.28% to 99.62% indicating a good D-AD experimental performance. The BMP value of CM was measured at 222.8 ± 4.4 NmL $CH_4$ $g_{VS}^{-1}$, this BMP was recovered at 98.66% on day 31. Monitoring of the volatile fatty acids, pH and buffer capacity did not evidenced inhibition problems during the D-AD process.

### *3.3.1 Biogas Production*

Similar behavior on methane production was observed for the four LBR compared with literature (Degueurce et al., 2016c; Riggio et al., 2017a), **Fig. 4a** presents the biogas and methane flow of the last reactor sacrificed at day 31. The first gas peak was observed around day 3, this was mainly carbon dioxide produced by aerobic digestion of rapid fermentative matter partially given the initial oxygen present in matter before the reactor sealing. Second gas peak production was achieved for all reactors between days 9 and 11. The valley between peaks 2 and 3 mark the slack on methane production. The third and last gas production peak was observed at day 16.5 ± 1.5 for the two remaining reactors. The cumulated methane for all reactors and the average production at the sacrificed days of still working reactors is depicted in **Fig. 4b**. Differences in methane production were attributed to the starting-up of the heating baths at the first moment of the experiment and to the experimental uncertainties. The results of methane production of these four LBR's were similar to the results presented by André et al. (2015) using recirculation each 2 h during 2 min with 100 L $h^{-1}$ of flow.

### *3.3.2 Cattle Manure Physical Characterizations at Different Stages of D-AD*

Physical characterization of cattle manure at different stages of D-AD process included the TS content, VS content, dry and wet bulk density and porosity and the WHC (**Table 2**). TS content decreased from 18.59 ± 0.43% to 11.10 ± 0.51% between the initial CM and the digestate at 31 days. VS consumption presented a linear behavior with time, probably matter degradation would have continued for some days more after day 31. Water impregnation and solid degradation

enhanced the augmentation of wet bulk density from 407.8 ± 14.1 to 914.2 ± 10.9 kg $m^{-3}$, in contrast, wet porosity values decreased from 51.7 ± 1.3 to 10.2 ± 1.5 % with time proving the bulk compaction with D-AD process with liquid recirculation. Dry values of bulk density and porosity did not present important changes as wet values (**Table 2**), thus water in samples plays an important role in physical characterization of CM and digestates. Similar results were obtained comparing the values of TS, VS, dry bulk density and dry porosity with the reported values by André et al. (2015). Otherwise, similarities between the values of the wet bulk density determined at the 60 L LBR's (data not shown) and those determined with the permeameter for WRC methodology were observed, meaning that the use of a 13 L permeameter did not inflect important changes in the structure of the digested biomass once this was sampled and placed in the permeameter.

### *3.3.3 WRC and porosity distribution of CM at different stages of D-AD in sacrificed LBR*

The WRC of CM and digested samples recovered at days 0, 10, 21 and 31 are depicted in **Fig. 5a**. In DA, the slope determining macropores in D-DA decreases with the anaerobic degradation of the solid medium. Initially, the macropores slope value in DA was -0.09, this value gradually decreased with the solid degradation, on day 10 the slope value was -0.059, at day 15 this was determined at -0.056, at day 21 was -0.029 and finally at day 31 the slope value was reduced until -0.006. Rapid mesopores (dashed yellow line) slopes presented lower variability than macropores slopes, they changed from -0.006 and -0.004 from days 0 to 31. TGA's results are also shown in **Fig. 5a**, as can be observed, the time of the test was slightly different for all samples even if the sample amount was the same in all performed TGA. In samples at day 0, the total humidity was removed in average 2865 seconds, this time increased at days 10 to 3150 seconds, degraded mater was able to hold more water, thus micropores volume increased from 16.2 ± 3.6% to 21.1 ± 3.9 in the first 10 days. After this point, micropores volume remains almost similar until the end of the experiment on day 31. Evaporation time was inferior on days

31 and 21, with 2670 and 2250 seconds, respectively. Moreover, water mass balance (Eq. **4**) values obtained for WRC analysis ranged from 88.3 ± 1.3 to 98.5 ± 2.2 % (**Table 2**), meaning a good WRC analysis performance.

Volume porosity distribution changes are depicted in **Fig 5b**. Macropores decreased linearly from 30 ± 3 on days 0 to 1.7 ± 0.3% on day 31, meaning a reduction of 94.3%. Macropores were converted into mostly mesopore volume which increased linearly from 44.4 ± 3.4 to 65.4 ± 0.2%. Moreover, micropores volume slightly increased from 16.2 ± 3.6 to 22.9 ± 0.3%. Previous results drive to a group of linear regression equations able to estimate the volumetric fractions of CM related in Eq. **(3)**. **Table 3** shows the slope (m) and the y-intercept which represent the initial percentages of macro, meso and micropores of CM. The use of these equations can allow the estimation of pores distribution changes of anaerobically digested CM between 0 and 31 days in 60 L LBR.

### *3.3.4 Effect of fiber degradation on pore distribution evolution and the permeability of the solid bed*

In this section the structural changes of the solid phase were related with fibers biological degradation. As defined before, CM is a mixture between cow feces and the wheat straw used as bedding material. The presence of wheat straw fibers gives a solid structure and high porosity values allowing the liquid percolation in LBR in the first days of batch. As a vegetal material, wheat straw is composed of fibers of cellulose, hemicellulose and lignin. Fiber content has been determined for samples from sacrificed D-AD reactors (**Fig. 6a**). Hemicellulose decreased from 27.2 ± 0.2 to 17.2 ± 0.6 $\%_{TS}$, whilst cellulose decreased from 31.9 ± 1.2 to 22.9 ± 1.0 $\%_{TS}$. The lignin is a non-degradable molecule by D-AD, thus, increase of the lignin content in the solid fraction was observed from 7.4 ± 0.2 % to 10.8 ± 0.5 $\%_{TS}$. **Table 3** depicts the linear regression parameters determining the kinetic degradation of hemicellulose and cellulose respectively, similar patterns of biological degradation were observed for both.

According to the Pearson correlation results between the pore distribution changes with fiber degradation and loss of permeability, macropores volume and the mass height were linearly related to the degradation of cellulose and hemicellulose content of the biomass. Strong correlations between these parameters were observed. Macropores reduction was correlated with hemicellulose and cellulose degradation in 0.98 and 0.93 respectively with p-values inferior to 0.05 (**Table 4**). Moreover, fiber degradation was found responsible for the loss of solid permeability from $2.5 \pm 0.2 \cdot 10^{-3}$ to $6.1 \pm 0.7 \cdot 10^{-5}$ m $s^{-1}$ (**Fig 6b**). The permeability was reduced in 97.6%, which is a very approximate value of the macropores reduction of 94.3% in 31 days of D-AD treatment of CM. Similar permeability reduction behavior was observed by André et al. (2015) in quantifying non-uniform flow using tracer experiments.

Methane production was well correlated with solid physical changes and fiber degradation with Pearson coefficient values higher than 0.79. Macropores volume reduction was strongly related to the settlement and compaction of the biomass with correlation coefficient of 0.98 (**Table 4**), indeed, the CM height was reduced from 42 ± 2 to 18.0 ± 0.4 cm in LBR between days 0 to 31, meaning height reduction of 57.1%. Hence, solid height decrease can be used as an indicator of macropores and permeability reduction. This consideration is important since at the industrial scale, following of the solid height would be easier than macropores and permeability; additionally, this does not entail the reactor sacrifice necessarily for solid sampling.

### *3.3.5 Implication of macropores reduction on the liquid recirculation operation in D-AD process*

In literature the positive effect of liquid recirculation on biogas production in LBR is well known (Degueurce et al., 2016b; Kusch et al., 2012). However, there is no clear consensus between the parameters leading liquid recirculation. In general, an operation mode is chosen once (total volume, frequency, flow) and is kept until the end of the batch operation without considering the physical changes occurred on the solid bed. André et al. (2015) has reported

poor percolation through the digestate on day 32, instead, liquid flow occurs at the reactor boundary, which is useless to keep moisture content inside the solid bed and to maintain solid degradation.

Since liquid percolation is possible due to the presence of macropores, the recirculated liquid volume should be adjusted according to the macropores reduction. This could enhance important reductions of energy consummation by recirculation pumps and extend their useful life period in industrial biogas production. In this work, approximately 40 L of liquid was discontinuously recirculated daily (2 minutes each 2 hours with flow 100 L/h), this recirculation mode was chosen for several reasons: the first 40 L was the initial solid working volume in the reactor, secondly, this recirculation mode has shown good D-AD performance for CM in previous research works (André et al., 2016, 2015). An alternative pattern of recirculation is shown in **Fig 6c**, here the daily recirculated volume is reduced considering the loss of macropores. Hitherto, none study about the effects of decreasing recirculation volume over D-AD has been found in literature. In this type of recirculation, only the liquid volume able to pass through the solid bed would be irrigated, avoiding excessive recirculation and liquid flow on the reactor boundary. Thus, the recirculated volume could be reduced in 50% in around 15 days (**Fig 6c**), and completely suppressed at day 31 in the treatment of CM.

## 4 Conclusion

D-AD using LBR system is often used in practice, while leaching pattern and strategy are not well understood. Therefore, characterization of the pore in the digestion medium is required. WRC analysis was useful to quantify the pore distribution of various raw solid biomasses into macro, meso and micropores. Solid compaction and loss of permeability during CM batch fermentation were related with the linear decrease of macropores and structural changes due to lignocellulosic fiber degradation. As macropores are essential to ensure percolation of the liquid,

the recirculated volume could be progressively reduced considering the kinetics of macropores volume decrease.

## 5 Supplementary material

Visual aspect of studied biomasses, liquid phase monitoring, reactor mass balances and Pearson correlation coefficients can be consulted as supplementary material.

## 6 Acknowledgments

The authors wish to thank the Agence Nationale Recherche Technologie (ANRT) for the financial support of this work and for the Ph.D. grant of Manuel HERNANDEZ-SHEK (CIFRE n° 2017/0352).

## 7 References

Abbassi-Guendouz, A., Brockmann, D., Trably, E., Dumas, C., Delgenès, J.-P., Steyer, J.-P., Escudié, R., 2012. Total solids content drives high solid anaerobic digestion via mass transfer limitation. Bioresour. Technol. 111, 55–61. https://doi.org/10.1016/j.biortech.2012.01.174

André, L., Durante, M., Pauss, A., Lespinard, O., Ribeiro, T., Lamy, E., 2015. Quantifying physical structure changes and non-uniform water flow in cattle manure during dry anaerobic digestion process at lab scale: Implication for biogas production. Bioresour. Technol. 192, 660–669. https://doi.org/10.1016/j.biortech.2015.06.022

André, L., Ndiaye, M., Pernier, M., Lespinard, O., Pauss, A., Lamy, E., Ribeiro, T., 2016. Methane production improvement by modulation of solid phase immersion in dry batch anaerobic digestion process: Dynamic of methanogen populations. Bioresour. Technol. 207, 353–360. https://doi.org/10.1016/j.biortech.2016.02.033

APHA, 2017. Standard methods for the examination of water and wastewater, 23rd ed, American Public Health Association. Inc. Washington, DC.

Brown, D., Shi, J., Li, Y., 2012. Comparison of solid-state to liquid anaerobic digestion of lignocellulosic feedstocks for biogas production. Bioresour. Technol. 124, 379–386. https://doi.org/10.1016/j.biortech.2012.08.051

Caicedo, L.M., Wang, H., Lu, W., De Clercq, D., Liu, Y., Xu, S., Ni, Z., 2017. Effect of initial bulk density on high-solids anaerobic digestion of MSW: General mechanism. Bioresour. Technol. 233, 332–341. https://doi.org/10.1016/j.biortech.2017.02.107

Darwish, T., 2009. Caractérisation des propriétés hydrodynamiques d'un sol de la Bekaa (Liban) sur les

588 rives du fleuve Litani. Étude Gest. des Sols 16, 67–84.
589 Degueurce, A., Clément, R., Moreau, S., Peu, P., 2016a. On the value of electrical resistivity tomography
590 for monitoring leachate injection in solid state anaerobic digestion plants at farm scale. Waste
591 Manag. 56, 125–136. https://doi.org/10.1016/j.wasman.2016.06.028
592 Degueurce, A., Tomas, N., Le Roux, S., Martinez, J., Peu, P., 2016b. Biotic and abiotic roles of leachate
593 recirculation in batch mode solid-state anaerobic digestion of cattle manure. Bioresour. Technol.
594 200, 388–395. https://doi.org/10.1016/j.biortech.2015.10.060
595 Degueurce, A., Trémier, A., Peu, P., 2016c. Dynamic effect of leachate recirculation on batch mode solid
596 state anaerobic digestion: Influence of recirculated volume, leachate to substrate ratio and
597 recirculation periodicity. Bioresour. Technol. 216, 553–561.
598 https://doi.org/10.1016/j.biortech.2016.05.113
599 Du, C., 2020. A novel segmental model to describe the complete soil water retention curve from
600 saturation to oven dryness. J. Hydrol. 584, 124649. https://doi.org/10.1016/j.jhydrol.2020.124649
601 Dumas, C., Silva Ghizzi Damasceno, G., Abdellatif, B., Carrère, H., Steyer, J.P., Rouau, X., 2015.
602 Effects of grinding processes on anaerobic digestion of wheat straw. Ind. Crops Prod. 74, 450–456.
603 https://doi.org/10.1016/j.indcrop.2015.03.043
604 Fernandez, H.C., Ramirez, D.A., Franco, R.T., Buffière, P., Bayard, R., 2020. Methods for the evaluation
605 of industrial mechanical pretreatments before anaerobic digesters. Molecules 25, 1–14.
606 https://doi.org/10.3390/molecules25040860
607 FranceAgrimer, 2016. L'observatoire national des ressources en biomasse - Évaluation des ressources
608 disponibles en France. Les études Fr.
609 Garcia-Bernet, D., Buffière, P., Latrille, E., Steyer, J.P., Escudié, R., 2011. Water distribution in
610 biowastes and digestates of dry anaerobic digestion technology. Chem. Eng. J. 172, 924–928.
611 https://doi.org/10.1016/j.cej.2011.07.003
612 Ge, X., Xu, F., Li, Y., 2016. Solid-state anaerobic digestion of lignocellulosic biomass: Recent progress
613 and perspectives. Bioresour. Technol. 205, 239–249. https://doi.org/10.1016/j.biortech.2016.01.050
614 Gerke, H.H., Van Genuchten, M.T., 1993. A dual-porosity model for simulating the preferential
615 movement of water and solutes in structured porous media. Water Resour. Res. 29, 305–319.
616 https://doi.org/10.1029/92WR02339
617 Gy, P.M., 1998. Sampling for Analytical Purposes 172.
618 Han, L., Feng, J., Zhang, S., Ma, Z., Wang, Y., Zhang, X., 2012. Alkali pretreated of wheat straw and its
619 enzymatic hydrolysis. Brazilian J. Microbiol. 43, 53–61. https://doi.org/10.1590/S1517-
620 83822012000100006
621 Holliger, C., Alves, M., Andrade, D., Angelidaki, I., Astals, S., Baier, U., Bougrier, C., Buffière, P.,
622 Carballa, M., De Wilde, V., Ebertseder, F., Fernández, B., Ficara, E., Fotidis, I., Frigon, J.C., De
623 Laclos, H.F., Ghasimi, D.S.M., Hack, G., Hartel, M., Heerenklage, J., Horvath, I.S., Jenicek, P.,
624 Koch, K., Krautwald, J., Lizasoain, J., Liu, J., Mosberger, L., Nistor, M., Oechsner, H., Oliveira,

J.V., Paterson, M., Pauss, A., Pommier, S., Porqueddu, I., Raposo, F., Ribeiro, T., Pfund, F.R., Strömberg, S., Torrijos, M., Van Eekert, M., Van Lier, J., Wedwitschka, H., Wierinck, I., 2016. Towards a standardization of biomethane potential tests. Water Sci. Technol. 74, 2515–2522. https://doi.org/10.2166/wst.2016.336

Jordan, A., Cerdá, A., 2010. Actualización en métodos y técnicas para el estudio de los suelos afectados por incendios forestales, in: València, U. de (Ed.), Actualización En Métodos y Técnicas Para El Estudio de Los Suelos Afectados Por Incendios Forestales. FUEGORED.

Karthikeyan, O.P., Visvanathan, C., 2013. Bio-energy recovery from high-solid organic substrates by dry anaerobic bio-conversion processes: A review. Rev. Environ. Sci. Biotechnol. 12, 257–284. https://doi.org/10.1007/s11157-012-9304-9

Klute, A., 1986. Water Retention: laboratory methods. Methods of soils analysis. Part 1. Physical and minerological methods. pp. 635–662.

Koch, K., Lübken, M., Gehring, T., Wichern, M., Horn, H., 2010. Biogas from grass silage - Measurements and modeling with ADM1. Bioresour. Technol. 101, 8158–8165. https://doi.org/10.1016/j.biortech.2010.06.009

Kusch, Sigrid, Kusch, S, Hans Oechsner, al, Jungbluth, T., 2012. Effect of various leachate recirculation strategies on batch anaerobic digestion of solid substrates. Int. J. Environ. Waste Manag. 1 J. Environ. Waste Manag. 9, 69–88. https://doi.org/10.1504/IJEWM.2012.044161

Lam, P.S., Sokhansanj, S., Bi, X., Lim, C.J., Naimi, L.J., Hoque, M., Mani, S., Womac, A.R., Ye, X.P., S., N., 2008a. Bulk density of wet and dry wheat straw and switchgrass particles. Appl. Eng. Agric. 24, 351–358. https://doi.org/10.13031/2013.24490

Lam, P.S., Sokhansanj, S., Bi, X., Mani, S., Lim, C.J., Womac, A.R., Hoque, M., Peng, J., JayaShankar, T., Naimi, L.J., Nayaran, S., 2008b. Physical characterization of wet and dry wheat straw and switchgrass – bulk and specific density. ASABE Annu. Int. Meet. 0300, 23. https://doi.org/10.13031/2013.24490

Lavelle, P., Moreira, F., Spain, A., 2014. Biodiversity: Conserving biodiversity in agroecosystems. Agric. food Syst.

Luxmoore, R.J., 1980. Micro-, Meso-, Macroporosity of Soil. Environ. Sci. Div. TN 37830, 671.

Menéndez, I., Caniego, J., Gallardo, J.F., Olechko, K., 2005. Use of fractal scaling to discriminate between and macro- and meso-pore sizes in forest soils, in: Ecological Modelling. pp. 323–335. https://doi.org/10.1016/j.ecolmodel.2004.04.009

Meng, X., Foston, M., Leisen, J., Demartini, J., Wyman, C.E., Ragauskas, A.J., 2013. Determination of porosity of lignocellulosic biomass before and after pretreatment by using Simons' stain and NMR techniques. Bioresour. Technol. 144, 467–476. https://doi.org/10.1016/j.biortech.2013.06.091

Møller, H.B., Moset, V., Brask, M., Riis Weisbjerg, M., Lund, P., 2014. Feces composition and manure derived methane yield from dairy cows: Influence of diet with focus on fat supplement and roughage type. Atmos. Environ. 94, 36–43. https://doi.org/10.1016/j.atmosenv.2014.05.009

Myint, M.T., Nirmalakhandan, N., 2008. Enhancing anaerobic hydrolysis of cattle manure in leach bed reactors. Bioresour. Technol. 100, 1695–1699. https://doi.org/10.1016/j.biortech.2008.09.031

Nishiyama, N., Yokoyama, T., 2017. Permeability of porous media: Role of the critical pore size. J. Geophys. Res. Solid Earth 122, 6955–6971. https://doi.org/10.1002/2016JB013793

Richards, L.A., 1948. Porous plate apparatus for measuring moisture retention and transmission by soil. Soil Sci. 66, 105–110.

Riggio, S., Hernandéz-Shek, M.A., Torrijos, M., Vives, G., Esposito, G., Van Hullebusch, E.D., Steyer, J.P., Escudié, R., 2017a. Comparison of the mesophilic and thermophilic anaerobic digestion of spent cow bedding in leach-bed reactors. Bioresour. Technol. 234, 466–471. https://doi.org/10.1016/j.biortech.2017.02.056

Riggio, S., Torrijos, M., Debord, R., Esposito, G., van Hullebusch, E.D., Steyer, J.P., Escudié, R., 2017b. Mesophilic anaerobic digestion of several types of spent livestock bedding in a batch leach-bed reactor: substrate characterization and process performance. Waste Manag. 59, 129–139. https://doi.org/10.1016/j.wasman.2016.10.027

Rocamora, I., Wagland, S.T., Villa, R., Simpson, E.W., Fernández, O., Bajón-Fernández, Y., 2020. Dry anaerobic digestion of organic waste: A review of operational parameters and their impact on process performance. Bioresour. Technol. 299, 122681. https://doi.org/10.1016/j.biortech.2019.122681

Sanchez, A., Hernández-Sánchez, P., Puente, R., 2019. Hydration of lignocellulosic biomass. Modelling and experimental validation. Ind. Crops Prod. 131, 70–77. https://doi.org/10.1016/j.indcrop.2019.01.029

Savitzky, A., Golay, M.J.E., 1964. Smoothing and Differentiation of Data by Simplified Least Squares Procedures. Anal. Chem. 36, 1627–1639. https://doi.org/10.1021/ac60214a047

Sawatdeenarunat, C., Surendra, K.C., Takara, D., Oechsner, H., Khanal, S.K., 2015. Anaerobic digestion of lignocellulosic biomass: Challenges and opportunities. Bioresour. Technol. 178, 178–186. https://doi.org/10.1016/j.biortech.2014.09.103

Shahriari, H., Warith, M., Hamoda, M., Kennedy, K.J., 2011. Effect of leachate recirculation on mesophilic anaerobic digestion of food waste. Waste Manag. 32, 400–403. https://doi.org/10.1016/j.wasman.2011.10.022

Shewani, A., Horgue, P., Pommier, S., Debenest, G., Lefebvre, X., Gandon, E., Paul, E., 2015. Assessment of percolation through a solid leach bed in dry batch anaerobic digestion processes. Bioresour. Technol. 178, 209–216. https://doi.org/10.1016/j.biortech.2014.10.017

Valencia, R., Van Der Zon, W., Woelders, H., Lubberding, H.J., Gijzen, H.J., 2008. The effect of hydraulic conditions on waste stabilisation in bioreactor landfill simulators. Bioresour. Technol. 100, 1754–1761. https://doi.org/10.1016/j.biortech.2008.09.055

Vallabh, R., Ducoste, J., Seyam, A.F., Banks-Lee, P., 2011. Modeling tortuosity in thin fibrous porous media using computational fluid dynamics. J. Porous Media 14, 791–804.

https://doi.org/10.1615/JPorMedia.v14.i9.40
Van Soest, P.J., 1963. Use of Detergents in the Analysis of Fibrous Feeds. II. A Rapid Method for the Determination of Fiber and Lignin. J. Assoc. Off. Agric. Chem. 46, 825–835.
Wassar, F., Gandolfi, C., Rienzner, M., Chiaradia, E.A., Bernardoni, E., 2016. Predicted and measured soil retention curve parameters in Lombardy region north of Italy. Int. Soil Water Conserv. Res. 4, 207–214. https://doi.org/10.1016/j.iswcr.2016.05.005
Yokoyama, T., Takeuchi, S., 2009. Porosimetry of vesicular volcanic products by a water-expulsion method and the relationship of pore characteristics to permeability. J. Geophys. Res. Solid Earth 114. https://doi.org/10.1029/2008JB005758

## Figures

**Fig. 1 (a)** Schematic pores structure of the biomass and definitions of pores function **(b)** Theoretical WRC with the test phases: Immersion and saturation (I&S), Drainage analysis (DA) and Thermogravimetric analysis (TGA)

**Fig. 2** Savitzky-Golay filter derivation over time of TGA results for RSG

**Fig. 3** WRC and porosity distribution for **(a)** Roadside grass (RSG), **(b)** Chopped corn stover (CCS) **(c)** Cattle Manure (CM) and **(d)** Shredded Cattle Manure (S-CM)

**Fig. 4 (a)** Specific biogas and methane flow in 60 L sacrificed batch reactors **(b)** Accumulated methane

**Fig. 5 (a)** WRC for CM treated in 60 L LBR's **(b)** Porosity distribution evolution of CM anaerobically digested

**Fig. 6 (a)** Fiber content degradation of CM **(b)** Permeability changes of CM **(c)** Reduction of daily recirculated volume with macropores evolution in D-AD

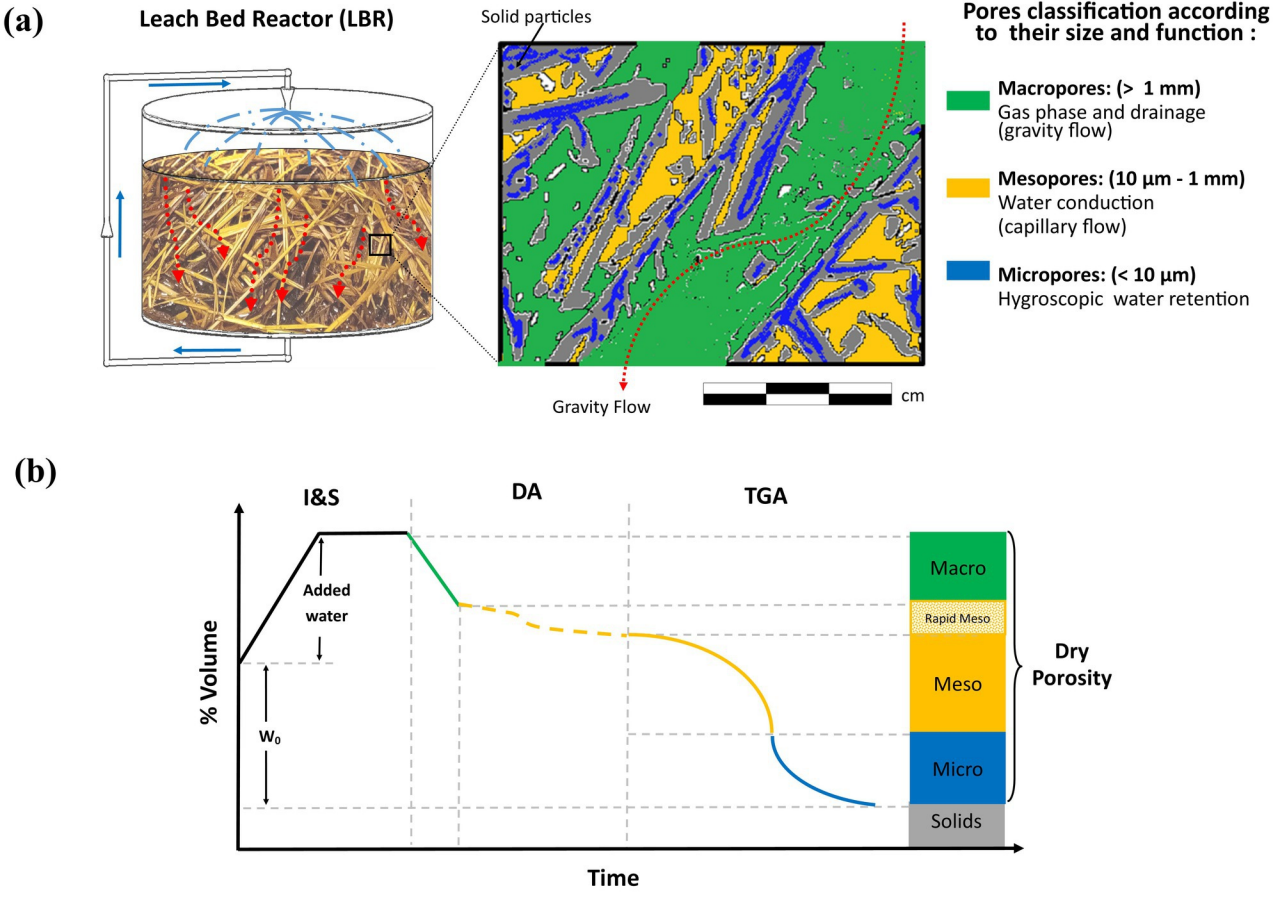
(a)
Leach Bed Reactor (LBR)
Solid particles
Pores classification according to their size and function :
Macropores: (> 1 mm)
Gas phase and drainage (gravity flow)
Mesopores: (10 µm - 1 mm)
Water conduction (capillary flow)
Micropores: (< 10 µm)
Hygroscopic water retention
Gravity Flow
cm
(b)
I&S
DA
TGA
Added water
% Volume
W0
Macro
Rapid Meso
Meso
Micro
Solids
Dry Porosity
Time

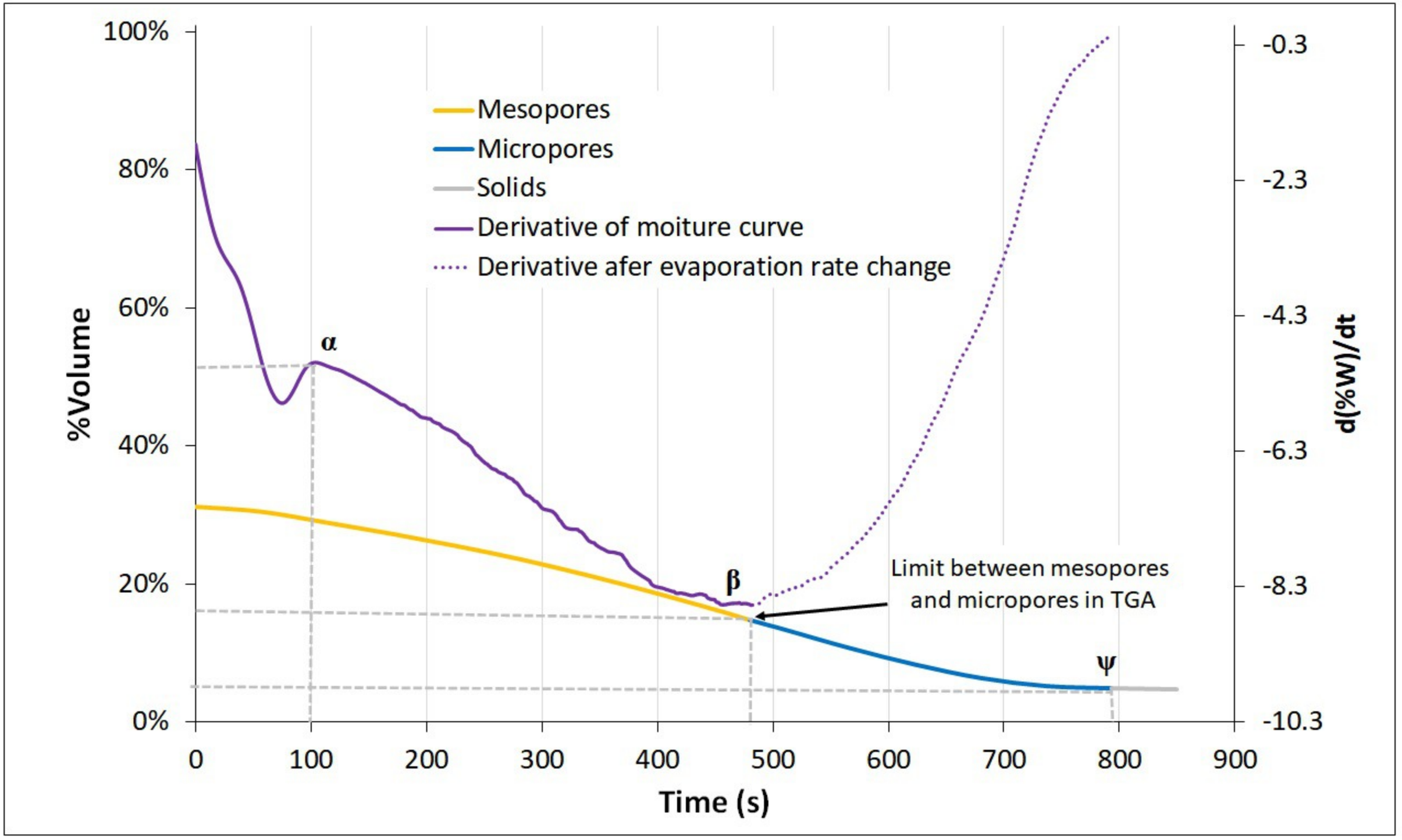
100%
80%
60%
40%
20%
0%
%Volume
-0.3
-2.3
-4.3
-6.3
-8.3
-10.3
d(%W)/dt
0
100
200
300
400
500
600
700
800
900
Time (s)
Mesopores
Micropores
Solids
Derivative of moiture curve
Derivative afer evaporation rate change
α
β
ψ
Limit between mesopores
and micropores in TGA

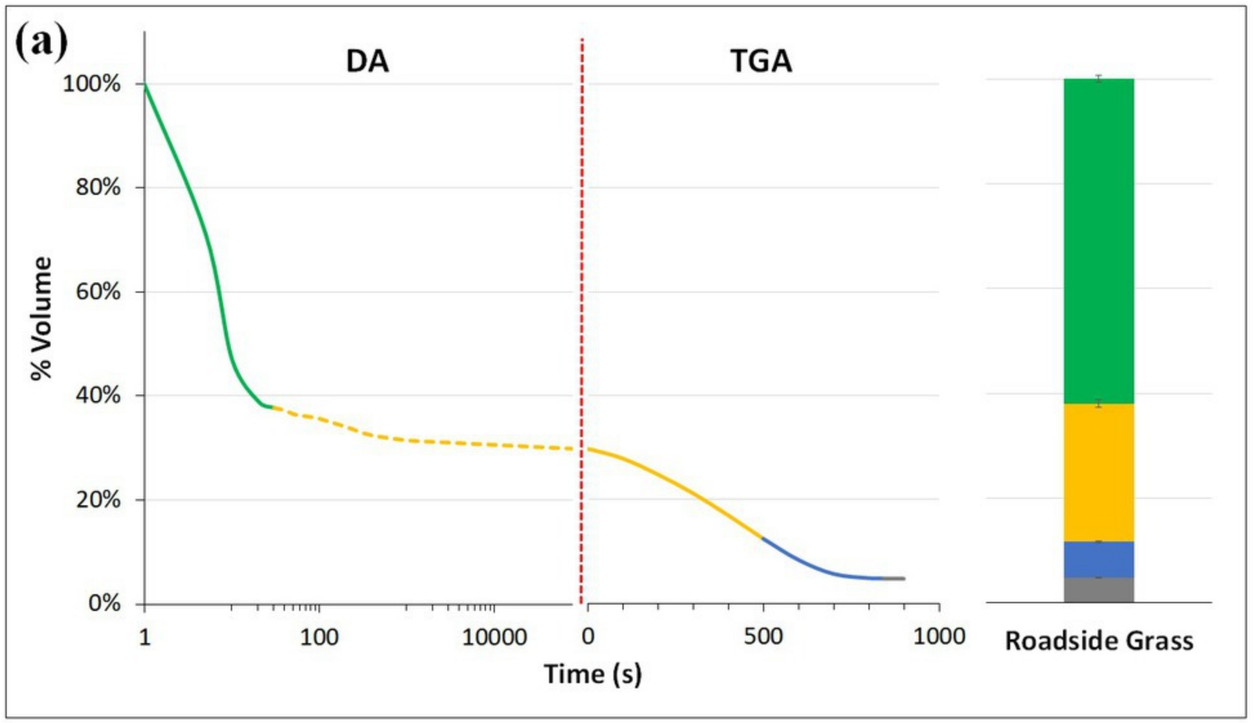


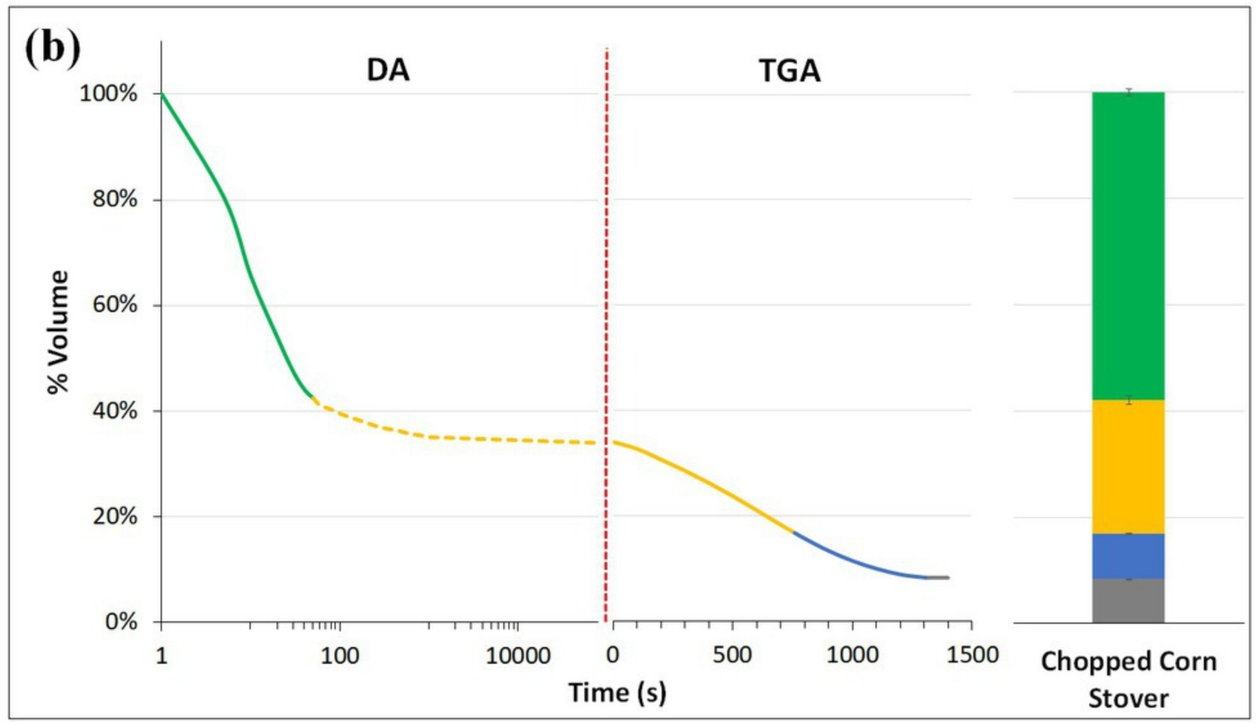


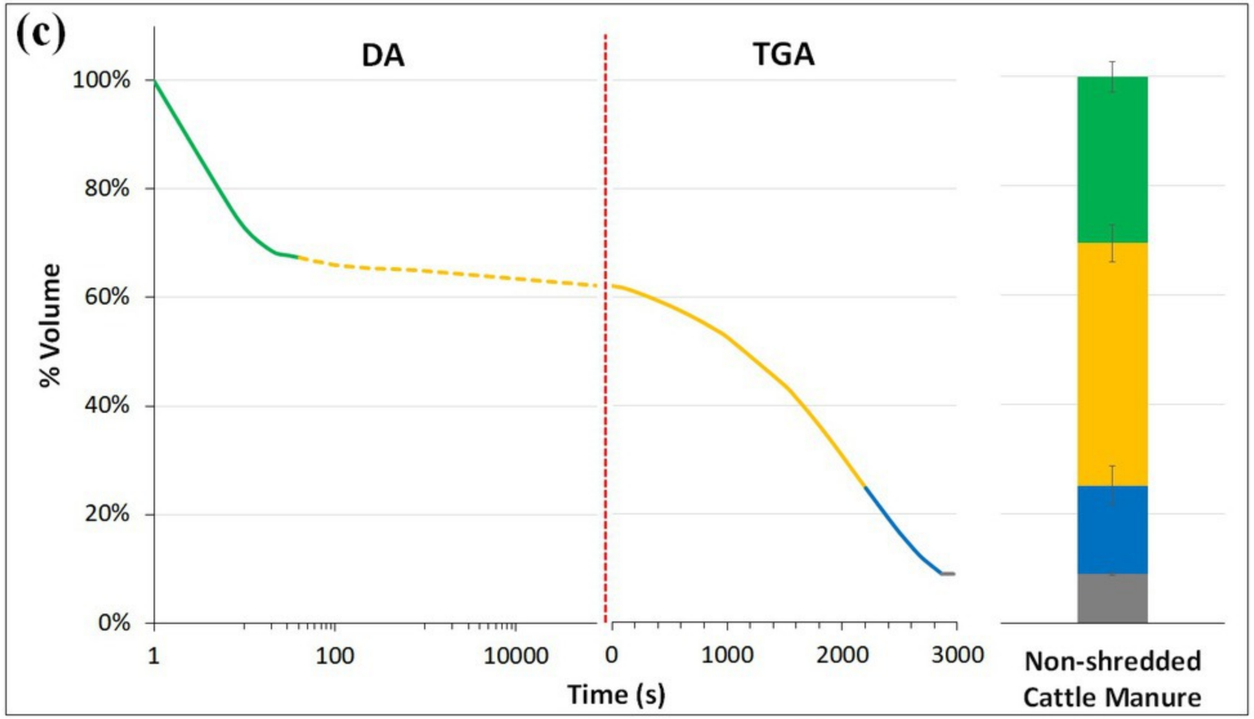


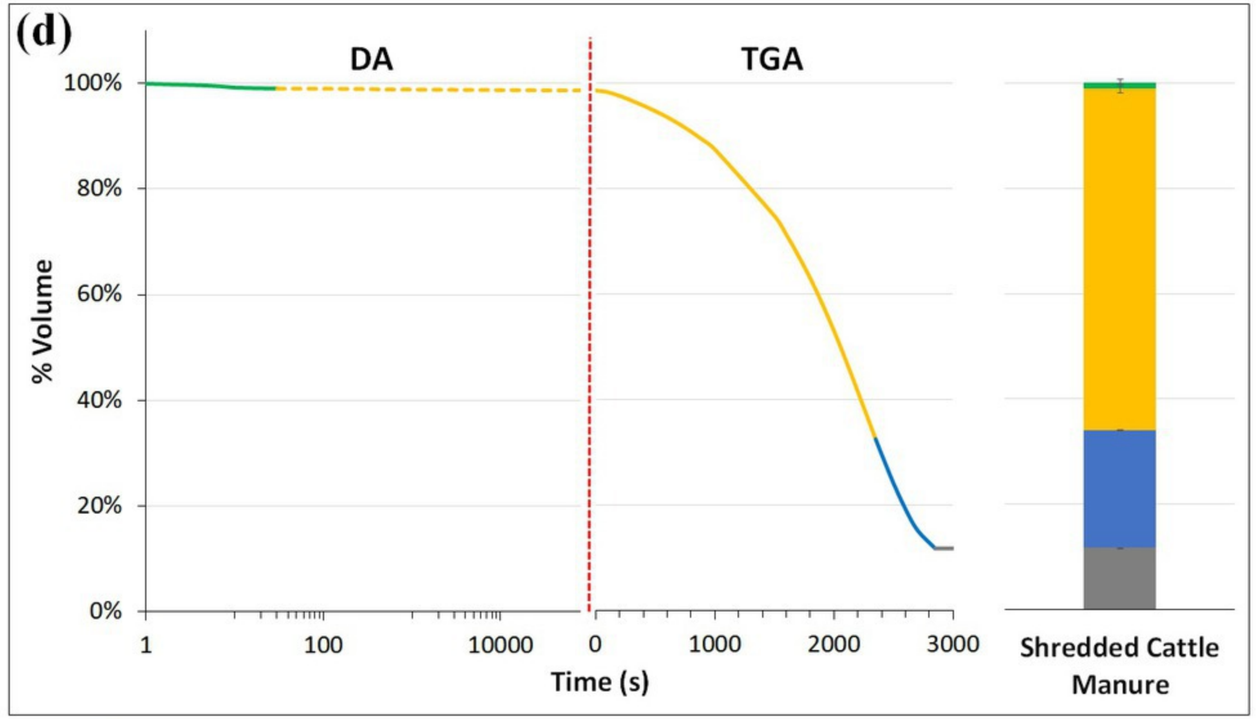


Macropores Mesopores Macropores Solids

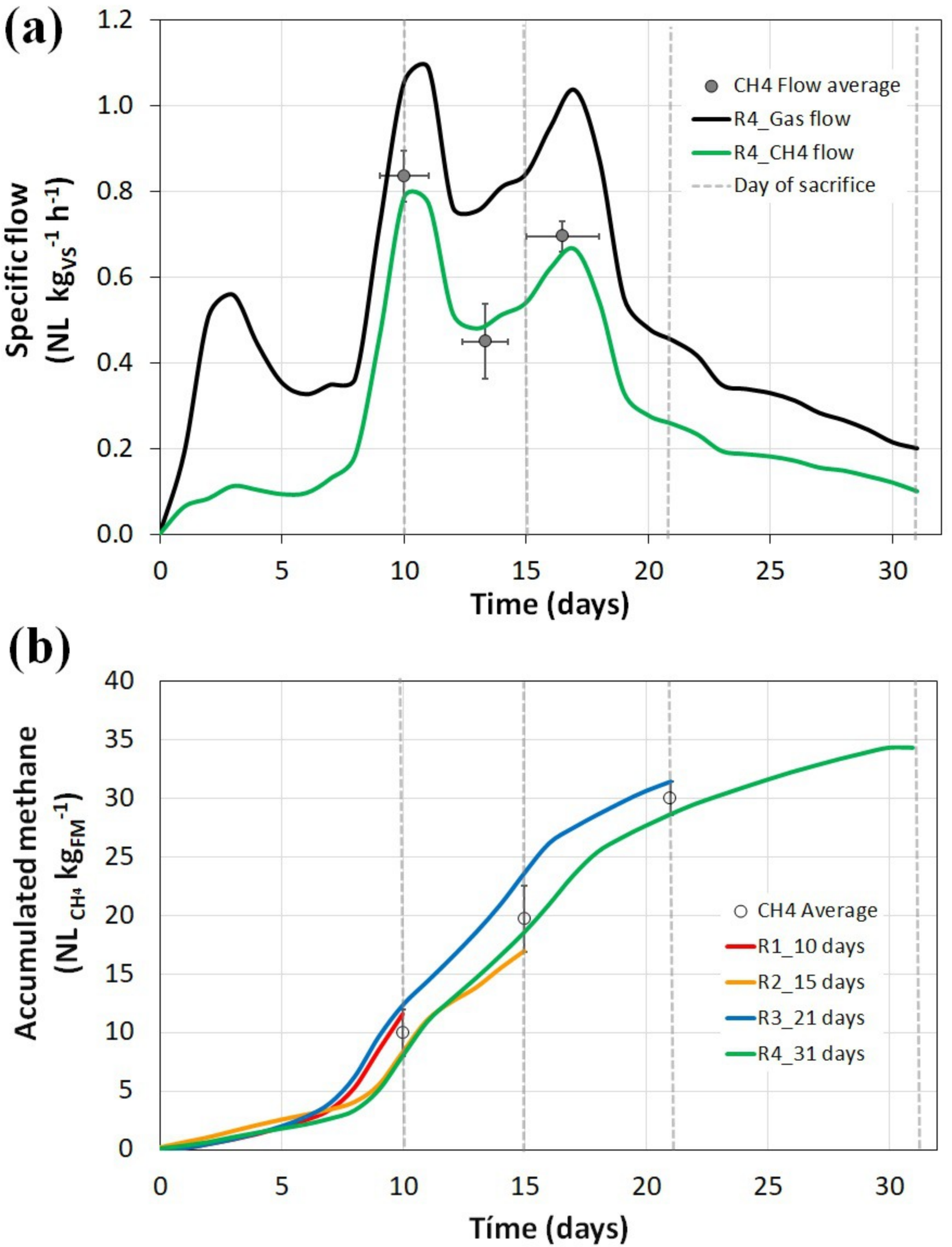
(a)
Specific flow (NL kgVS-1 h-1)
1.2
1.0
0.8
0.6
0.4
0.2
0.0
0
5
10
15
20
25
30
Time (days)
CH4 Flow average
R4_Gas flow
R4_CH4 flow
Day of sacrifice
(b)
Accumulated methane (NL CH4 kgFM-1)
40
35
30
25
20
15
10
5
0
0
5
10
15
20
25
30
Time (days)
CH4 Average
R1_10 days
R2_15 days
R3_21 days
R4_31 days

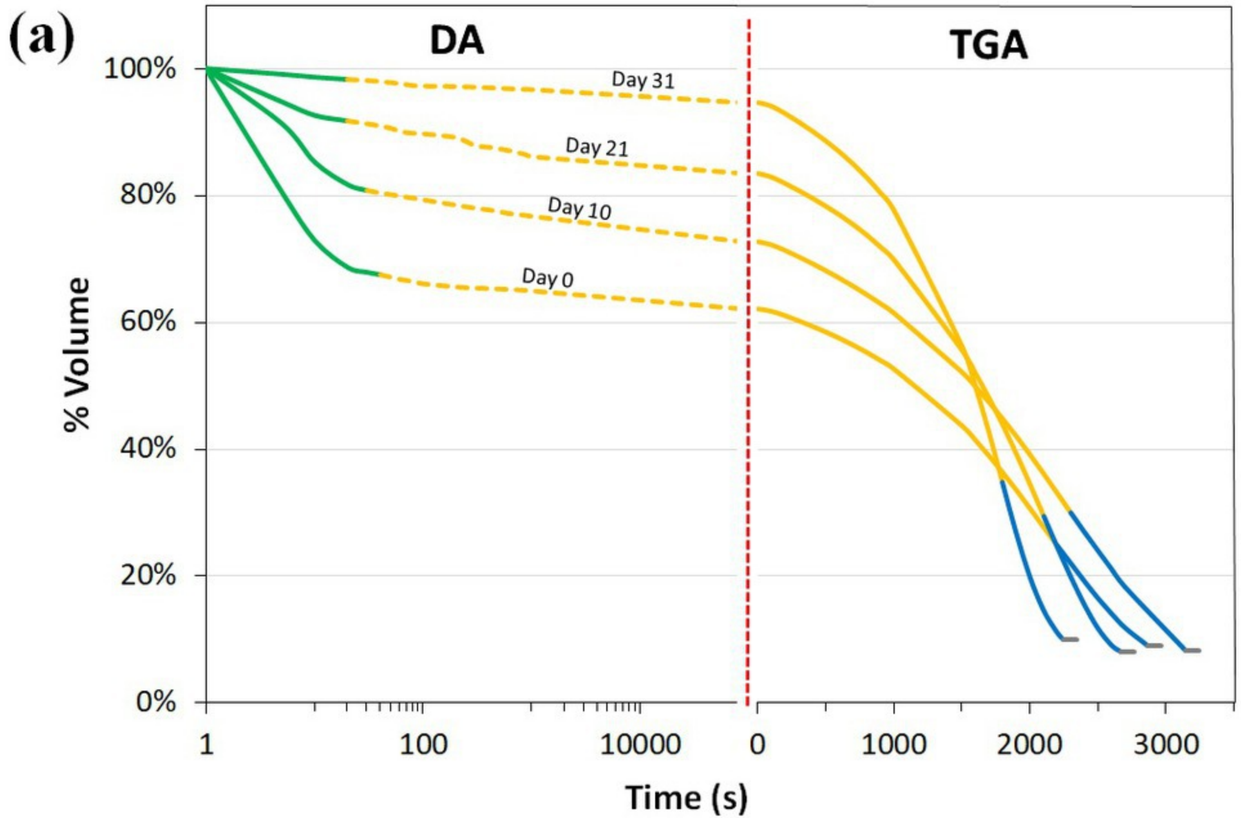
(a)
DA
TGA
Day 31
Day 21
Day 10
Day 0
100%
80%
60%
40%
20%
0%
% Volume
1
100
10000
0
1000
2000
3000
Time (s)

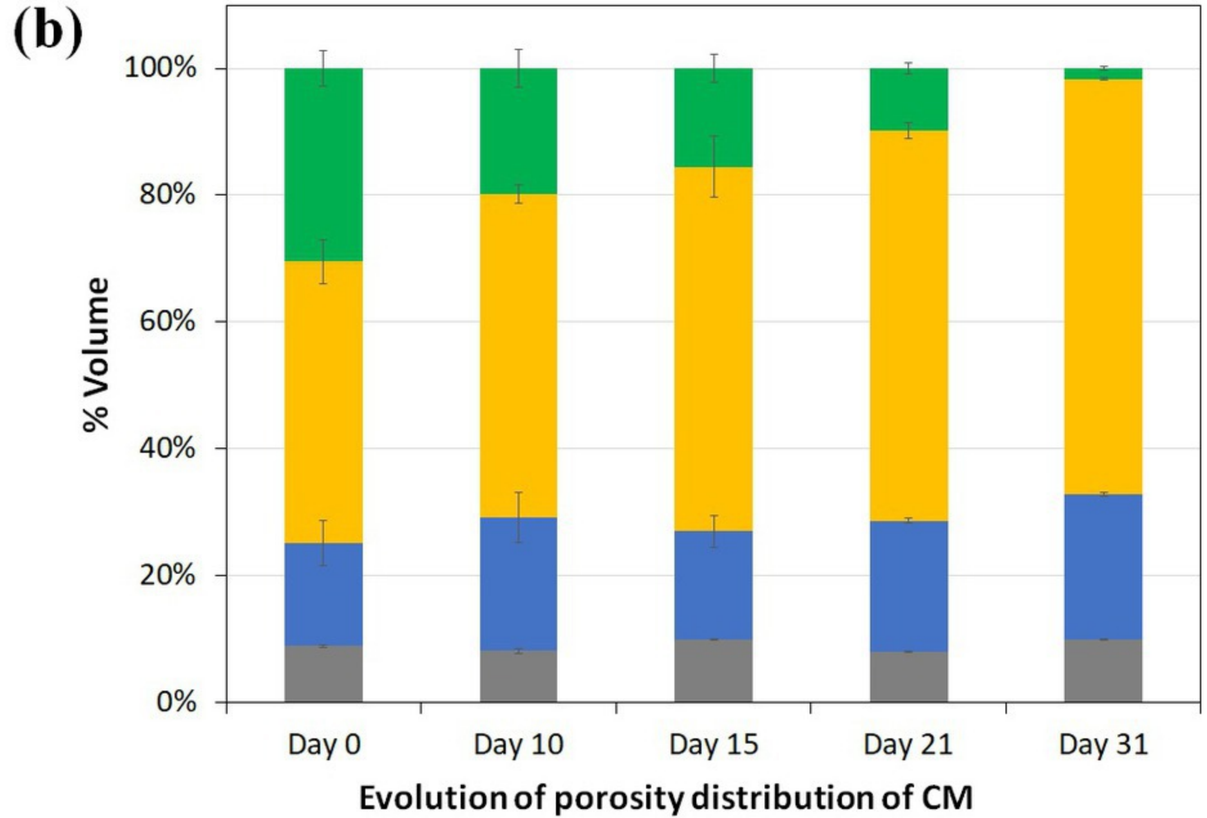
(b)
100%
80%
60%
40%
20%
0%
% Volume
Day 0
Day 10
Day 15
Day 21
Day 31
Evolution of porosity distribution of CM

(a)

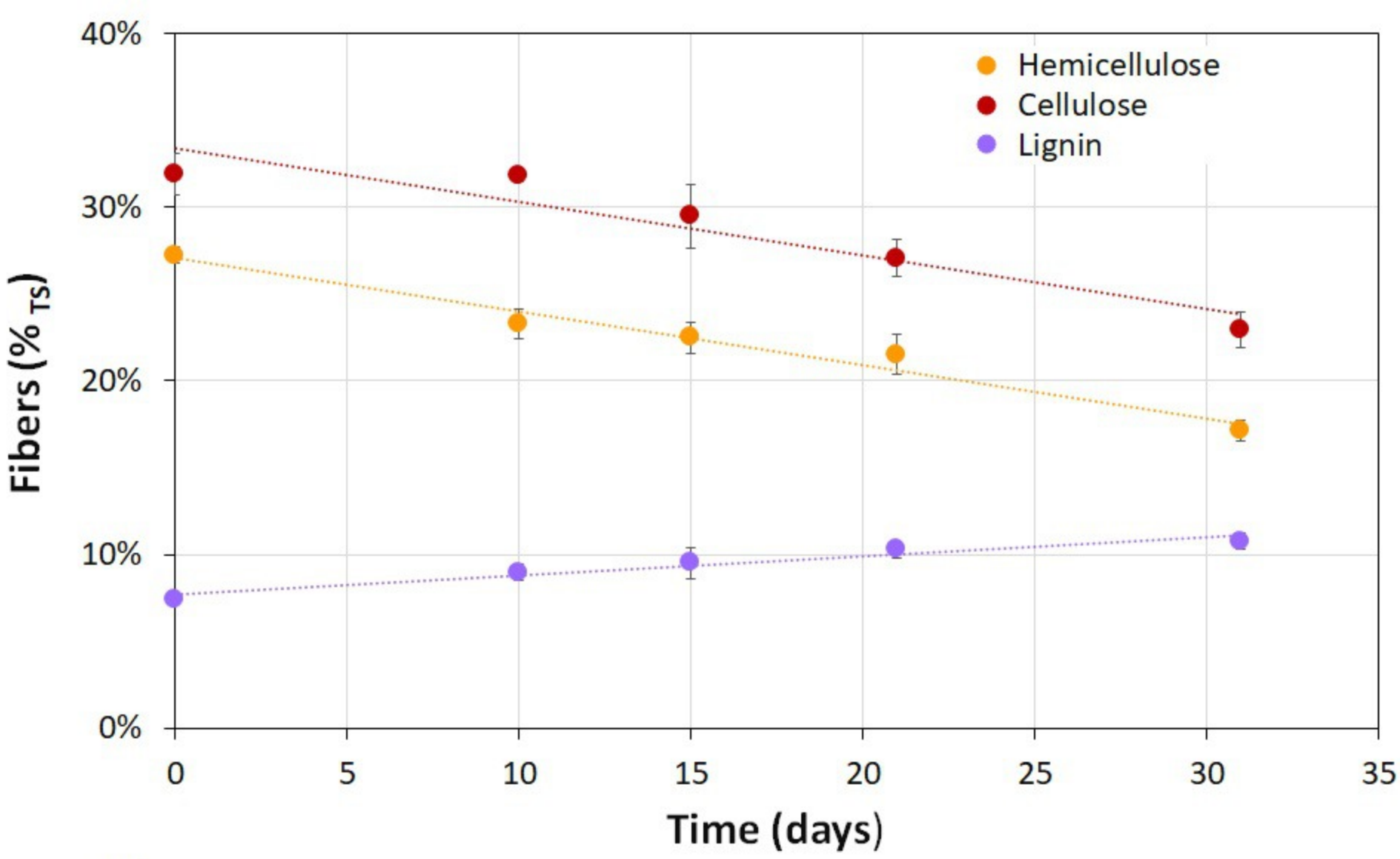
Hemicellulose
Cellulose
Lignin
Fibers (% TS)
40%
30%
20%
10%
0%
0
5
10
15
20
25
30
35
Time (days)

(b)

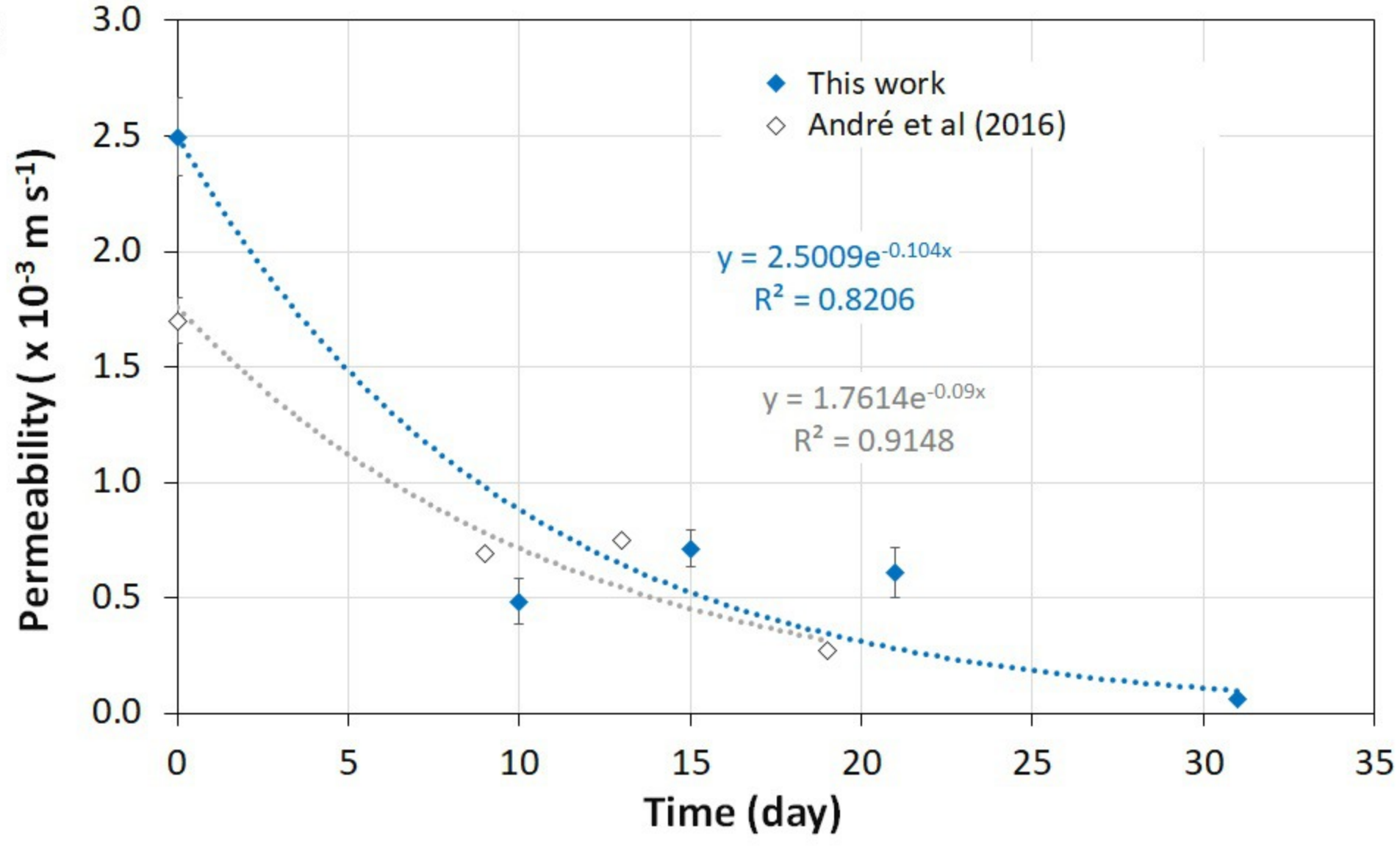
This work
André et al (2016)
y = 2.5009e-0.104x
R² = 0.8206
y = 1.7614e-0.09x
R² = 0.9148
Permeability ( x 10-3 m s-1)
3.0
2.5
2.0
1.5
1.0
0.5
0.0
0
5
10
15
20
25
30
35
Time (day)

(c)

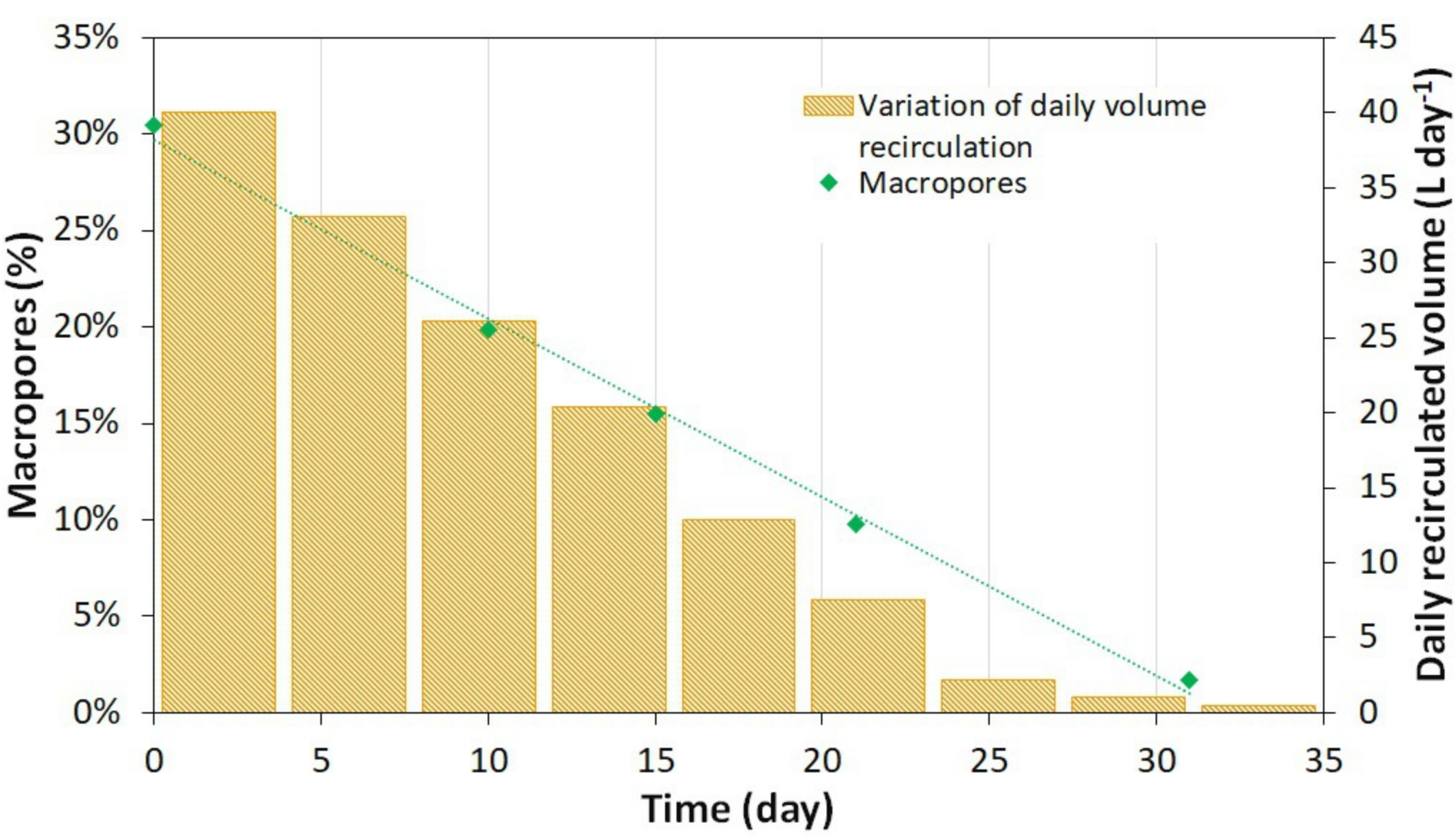
Variation of daily volume recirculation
Macropores
Macropores (%)
35%
30%
25%
20%
15%
10%
5%
0%
Daily recirculated volume (L day-1)
45
40
35
30
25
20
15
10
5
0
0
5
10
15
20
25
30
35
Time (day)

**Table 1.** Biomass characterization

| Biomass | RSG | CCS | S-CM | CM |
|---|---|---|---|---|
| **Particle shape** | Plate | Angular | Plate | Cylindrical |
| **Particle size** | Length: 10-15 cm<br>Thickness: <2 mm | 1-2 cm | Length: <5 cm<br>Thickness: <2 mm | Length: 10-20 cm<br>Diameter: <5 mm |
| **TS (%)** | 22.6 ± 0.6 | 37.9 ± 0.6 | 14.5 ± 1.7 | 18.6 ± 0.4 |
| **VS ($\%_{TS}$)** | 85.3 ± 0.6 | 95.8 ± 0.7 | 79.4 ± 1.5 | 86.4 ± 0.1 |
| **$\rho_{wet}$ (kg $m^{-3}$)** | 174.1 ± 4.5 | 166.2 ± 0.7 | 797.8 ± 11.4 | 407.8 ± 14.1 |
| **$\rho_{dry}$ (kg $m^{-3}$)** | 39.4 ± 1.0 | 63.0 ± 0.3 | 115.6 ± 1.7 | 75.8 ± 2.6 |
| **$\varepsilon_{wet}$ (%)** | 78.7 ± 0.1 | 77.9 ± 0.4 | 18.6 ± 1.7 | 51.7 ± 1.3 |
| **$\varepsilon_{dry}$ (%)** | 95.2 ± 0.1 | 91.6 ± 0.1 | 88.2 ± 0.3 | 91.0 ± 0.2 |
| **$\theta_{mobile}$/ $\theta_{added}$ (%)** | 76.1 ± 0.8 | 73.7 ± 2.3 | 5.5 ± 1.0 | 60.0 ± 3.6 |
| **$\theta_{mobile}$/ $\theta_{total}$ (%)** | 62.9 ± 0.6 | 62.6 ± 2.2 | 1.2 ± 0.1 | 33.5 ± 2.7 |
| **WHC ($g_{water}$ $g_{DM}^{-1}$)** | 7.4 ± 0.1 | 4.1 ± 0.2 | 7.4 ± 0.2 | 6.7 ± 0.2 |
| **WMB (%)** | 96.7 ± 0.1 | 99.0 ± 0.8 | 99.0 ± 0.2 | 98.5 ± 2.2 |
| **K (m $s^{-1}$)** | $1.3 \pm 0.3 \cdot 10^{-3}$ | $8.6 \pm 0.6 \cdot 10^{-4}$ | $1.2 \pm 0.2 \cdot 10^{-8}$ | $2.5 \pm 0.2 \cdot 10^{-3}$ |

**Table 2.** Physical characteristics evolution of digested CM

| Event | CM_Day 0 | CM_Day 10 | CM_Day 15 | CM_Day 21 | CM_Day 31 |
|---|---|---|---|---|---|
| **TS (%)** | 18.6 ± 0.4 | 11.7 ± 0.1 | 13.9 ± 0.1 | 10.5 ± 0.3 | 11.1 ± 0.5 |
| **VS ($\%_{TS}$)** | 86.4 ± 0.1 | 82.7 ± 0.2 | 82.1 ± 0.3 | 78.6 ± 0.2 | 76.0 ± 0.3 |
| **$\rho_{wet}$ (kg $m^{-3}$)** | 407.8 ± 14.1 | 556.0 ± 4.0 | 594.6 ± 13.8 | 766.2 ± 15.3 | 914.2 ± 0.9 |
| **$\rho_{dry}$ (kg $m^{-3}$)** | 75.8 ± 2.6 | 64.8 ± 0.5 | 82.9 ± 1.9 | 80.6 ± 1.6 | 101.5 ± 1.2 |
| **$\varepsilon_{wet}$ (%)** | 51.7 ± 1.3 | 29.8 ± 3.2 | 28.4 ± 0.2 | 23.9 ± 1.1 | 10.2 ± 1.5 |
| **$\varepsilon_{dry}$ (%)** | 91.0 ± 0.2 | 91.8 ± 0.4 | 90.0 ± 0.1 | 92.0 ± 0.1 | 90.0 ± 0.2 |
| **WHC ($g_{water}$ $g_{DM}^{-1}$)** | 6.7 ± 0.2 | 8.9 ± 0.1 | 7.5 ± 0.3 | 10.4 ± 0.3 | 8.9 ± 0.2 |
| **WMB (%)** | 98.5 ± 2.2 | 95.1 ± 0.1 | 95.3 ± 4.6 | 88.3 ± 1.3 | 96.6 ± 0.7 |

**Table 3.** Evolution of linear regression parameters for CM treated in sacrificed batch LBR's

| | Parameter (y) | m | $y_0$ | $R^2$ |
|---|---|---|---|---|
| **Porosity distribution (% Total volume)** | **Macropores** | -0.0090 | 0.2945 | 0.99 |
| | **Mesopores** | 0.0068 | 0.4529 | 0.96 |
| | **Micropores** | 0.0019 | 0.1665 | 0.61 |
| **Fiber content (%TS)** | **Hemicellulose** | -0.0310 | 0.2705 | 0.97 |
| | **Cellulose** | -0.0031 | 0.3337 | 0.89 |
| | **Lignin** | 0.0110 | 0.0772 | 0.95 |
| **Compaction** | **Height (m)** | -0.0081 | 0.4026 | 0.93 |
| | **Wet bulk density (kg $m^{-3}$)** | 16.69 | 390.76 | 0.98 |

**Table 4.** Results linear regression comparing the results of characterization of digested CM

| Parameters | Coefficient R | p-value | Confidence level |
|---|---|---|---|
| VS ↔ Hemicellulose | 0.97 | $6.17 \cdot 10^{-3}$ | 95% |
| VS ↔ Cellulose | 0.94 | $1.94 \cdot 10^{-2}$ | 95% |
| Hemicellulose ↔ Macropores | 0.98 | $2.56 \cdot 10^{-3}$ | 95% |
| Cellulose ↔ Macropores | 0.93 | $2.36 \cdot 10^{-2}$ | 95% |
| Macropores ↔ Solid Height | 0.98 | $4.37 \cdot 10^{-3}$ | 95% |
| Macropores ↔ Permeability | 0.87 | $5.56 \cdot 10^{-2}$ | 90% |

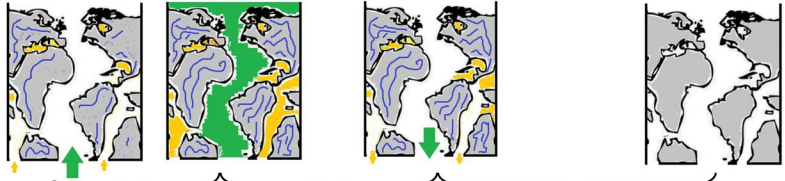

Immersion and Saturation (I&S)

Draining Analysis (DA)

Thermogravimetric Analysis (TGA)

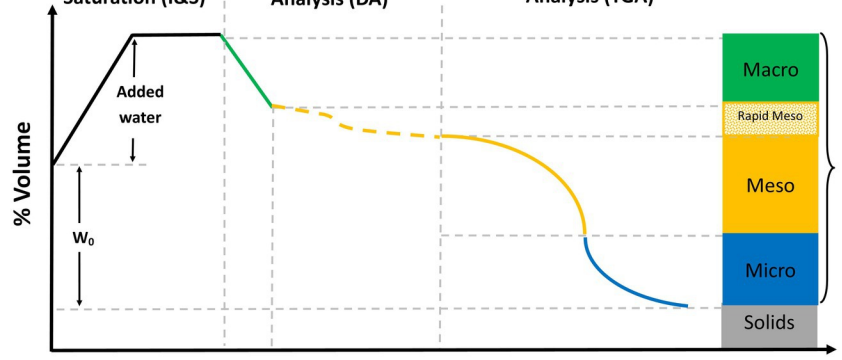


**Dry Porosity**

**Biomass pore classification**

- **Macropores: (> 1 mm)** Gas phase and drainage (gravity flow)
- **Mesopores: (10 µm - 1 mm)** Water conduction (capillary flow)
- **Micropores: (< 10 µm)** Hygroscopic water retention